Ecological Informatics 41 (2017) 91–107

Contents lists available at ScienceDirect

Ecological Informatics

journal homepage: www.elsevier.com/locate/ecolinf

Towards the development of an ecophysiological *Daphnia* model to examine effects of toxicity and nutrition

Felicity J. Ni, Noreen E. Kelly, George B. Arhonditsis*

Department of Physical and Environmental Sciences, University of Toronto, 1065 Military Trail, Toronto, Ontario M1C 1A4, Canada

ARTICLE INFO

Keywords:
Mercury
Metabolomics
Nutrition
Zooplankton
Ecophysiology
Environmental health
Modelling

ABSTRACT

Freshwater ecosystems are highly susceptible to mercury (Hg) deposition, which impacts biotic health and leads to serious consequences through biomagnification. The keystone zooplankter, *Daphnia*, exerts disproportionate effects on food web dynamics, displaying high sensitivity to natural stressors, and thus serving as an indicator of the broader impairments of aquatic ecosystems. Combined with metabolomics, the study of metabolites and their chemical processes, we have developed a model that attempts to elucidate the interactive effects of Hg toxicity and nutrition on phytoplankton-*Daphnia* relationships. Our model stipulates a physiological hierarchy, prioritizing different metabolic processes in the order of neurological functions, bioenergetics, osmoregulatory maintenance, waste management, and growth investments. *Daphnia* resilience is controlled by both food quantity and quality and each physiological process is modulated by the somatic levels of different metabolites. By enriching food with metabolites associated with neurological and energetic physiological pathways, effects of toxicity can be alleviated. Specifically, we demonstrate that metabolites associated with bioenergetics (carbohydrates, fats, proteins, and phosphorus) confer the greatest resilience to physiological changes induced by toxicity. Prey-predator dynamics can change significantly due to the detrimental impacts of toxicity on daphnid physiology and unfavourable nutritional stoichiometry. Under conditions of poor nutrition and extreme toxicity, our model demonstrates that daphnid populations may collapse and thus phytoplankton could escape intense grazing pressure. Founded upon the premise that response to stress can be more rapidly detected at the metabolic level, our study offers a new perspective to develop bioindicator systems and early warning signals for more efficient environmental monitoring.

1. Introduction

Despite over 30 years of efforts to control anthropogenic mercury (Hg) emissions, it has recently re-emerged as a contaminant of concern, particularly in North America (Gilbertson and Carpenter, 2004). Concerns are centered around methylmercury (MeHg), a bioavailable species of Hg that is a potent and highly toxic contaminant in aquatic systems (Zananski et al., 2011). MeHg enters the aquatic food web through direct uptake of water and ingestion of contaminated food by aquatic organisms (Chen and McNaught, 1992). At the base of the food web, uptake of MeHg occurs through passive transfer when phytoplankton uptake MeHgCl (Watras et al., 1998) and through active transfer when algal cells use energy to take up compounds that are bound with MeHg (Pickhardt and Fisher, 2007). MeHg may form complexes with ingested nutrients; for instance, MeHg has been found to form complexes with molecules such as cysteine and certain proteins due to its affinity for sulfhydryl groups (Roos et al., 2010). Because of this chemical property, MeHg possesses a strong affinity for muscle tissues where it bioaccumulates at higher trophic levels (Zananski et al., 2011). Subsequently, MeHg can biomagnify, with a bioaccumulation factor of about 10^7, achieving toxic levels at the top of the aquatic food web (Driscoll et al., 2007; Kim et al., 2014).

Zooplankton play a significant role in transferring MeHg from the base of food chains to higher trophic levels in freshwater ecosystems (Pickhardt et al., 2005; Tsui and Wang, 2004). Phytoplankton Hg sequestration results in intracellular concentrations that are 10^4 to 10^6 times greater than ambient water levels (Pickhardt et al., 2005). The consumption of contaminated phytoplankton by herbivorous zooplankton, such as *Daphnia*, and their inefficient excretion of MeHg, subsequently leads to the transfer of MeHg to higher trophic levels (Tsui and Wang, 2004). As fish obtain most of their Hg through dietary sources, zooplankton communities may thus play a major role in the bioaccumulation of Hg in fish (Pickhardt et al., 2005). Similarly, Rolfhus et al.'s (2011) analysis of bioaccumulation and biomagnification factors between water, seston, zooplankton, and fish identified that the greatest accumulation of MeHg took place at the lower trophic levels. Further-

* Corresponding author.
E-mail address: georgea@utsc.utoronto.ca (G.B. Arhonditsis).

http://dx.doi.org/10.1016/j.ecoinf.2017.04.002
Received 10 January 2017; Received in revised form 9 April 2017; Accepted 12 April 2017
Available online 13 April 2017
1574-9541/ © 2017 Elsevier B.V. All rights reserved.

more, Westcott and Kalff (1996) found that MeHg levels in zooplankton and fish of the same lakes were well correlated, suggesting that lower trophic levels, such as zooplankton, may be indicative of the relative Hg bioavailability throughout the food web. Much of the current literature on Hg toxicity in *Daphnia* focuses on mortality and reproductive losses, suggesting a knowledge gap of the role of MeHg in lower trophic levels. Clearly, there is a critical need to better understand the role of lower trophic levels in the propagation of MeHg in aquatic systems.

Previous research has highlighted the impacts of toxic metals at the molecular level by drawing upon the emerging field of metabolomics (e.g., García-Sevillano et al., 2014) and studying the consequences of toxicity on organismal physiology. Metabolomics, the study of low-weight biomolecules (< 1000 Da) within cells, tissues, and fluids of organisms, has emerged as a valuable avenue to gain insights into the biochemistry and physiology of organisms (García-Sevillano et al., 2014). Environmental metabolomics specifically focus on using information regarding important metabolites to understand interactions between organisms and their environment (García-Sevillano et al., 2014). Metabolic responses to stressors at the level of an individual organism can then be used to infer about the dynamics at higher levels of ecological organization via a bottom-up approach (Lankadurai et al., 2013; Perhar et al., 2016). Thus, by combining our knowledge of metabolomics and contaminant exposure, we can develop predictive tools to be used in the area of environmental management (e.g., Perhar and Arhonditsis, 2015). *Daphnia* plays a crucial role in aquatic ecosystems at the primary producer-grazer interface, linking autotrophs to higher trophic levels, and has been identified as a keystone species, where the state of the individual can be a reliable indicator of the ecosystem state (Brett and Müller-Navarra, 1997; Miner et al., 2012). In exposure experiments with metals, *Daphnia magna* metabolite composition showed significant changes at sub-lethal concentrations (Nagato et al., 2013). The concentrations of several amino acids, most notably those involved in the Krebs cycle decreased following exposure, indicating either slower production or accelerated exhaustion of amino acids to avoid toxicity. Nagato et al. (2013) found that exposure to metals such as copper, lithium, and arsenic can impact neurotransmitter synthesis and impair bioenergetics. Reproduction is also impacted as evidenced by empirical studies demonstrating the toxic effects of MeHg leading to lethality and reduction in net reproduction of *D. magna* (Chen and McNaught, 1992).

Diet quality through nutrition has been identified as a mediator in the reduction of Hg trophic transfer. Recently, there has been growing interest in the somatic growth dilution (SGD) effect on toxicants. This effect postulates that rapid growth can reduce bioaccumulation and MeHg trophic transfer. Karimi et al. (2007) report that daphnids consuming high quality algal food had MeHg concentrations significantly lower than those fed upon low quality algae. *Daphnia* exhibited a proportionately greater biomass gain as compared to MeHg increase due to elevated growth rates and reduced ingestion rates (Karimi et al., 2007). Similarly, algal bloom dilution has been explored as a means to reduce Hg bioaccumulation, as well as other metals (Pickhardt et al., 2005). As algal biomass increases, Hg concentration per algal cell decreases and consumers ingest and accumulate less Hg. Pickhardt et al. (2005) examined the role of zooplankton composition and phytoplankton abundance on Hg accumulation in zooplankton. Taxonomic composition and phosphorus levels, which mediated algal abundance, contributed to the majority of the variance in zooplankton MeHg concentrations. Chen et al. (2012) further corroborate the dilution of Hg at lower trophic levels in eutrophic water bodies due to the higher phytoplankton biovolume and density (Chen et al., 2012), although the same conditions could conceivably lead to a lower zooplankton to phytoplankton ratio due to higher abundance of inferior quality phytoplankton, such as cyanobacteria (Heathcote et al., 2016).

Perhar and Arhonditsis (2015) developed a zooplankton ecophysiology model inspired by *Daphnia* metabolomics data to link metabolites to physiological processes and ultimately draw inference regarding the health of the individual. The model simulated physiological processes within *Daphnia* and demonstrated the effects of nutritional shifts: unbalanced diets had profound implications on daphnid homeostasis as a result of elevated energetic requirements. Further, Perhar and Arhonditsis (2015) demonstrated that under differing homeostatic strategies, the allocation of energy varied due to the daphnid prioritizing certain processes; for instance, with a high maintenance strategy, daphnids allotted more resources to regulatory turnover and maintenance, rather than growth. Following this work, Perhar et al. (2016) coupled the ecophysiology sub-model with a Lotka-Volterra model to examine how variations in resource allocations affect zooplankton growth and subsequently phytoplankton dynamics. The same study highlighted the emergence of abrupt shifts between alternative states induced by variations in both food quantity and quality (Perhar et al., 2016). Overall, the introduction of zooplankton ecophysiology into a prey-predator system demonstrated how microscopic processes at the organismal level can be connected to macroscopic patterns and shape trophodynamics.

In this study, we present a *Daphnia* ecophysiology model, based on the developments by Perhar and Arhonditsis (2015) and Perhar et al. (2016), which explicitly incorporates MeHg exposure. Specifically, our model examines the neurological, reproductive, and waste management costs associated with MeHg exposure on *Daphnia* physiology and subsequent ecosystem states. We set out to address the following questions and predictions:

- How does the response of our predator-prey system differ in terms of resistance and resilience when exposed to MeHg? We define resistance as the ability of a predator-prey system to avoid changes. The resilience of phytoplankton and daphnid populations is determined by the ability to recover from a stressful exposure event. Low resilience is considered to be no recovery after MeHg exposure, where recovery is defined as the return of populations to qualitatively similar levels of biomass, prior to an exposure or stressor event. We expect the resilience of the system and resistance of daphnid populations to decrease significantly under scenarios of MeHg exposure.
- What is the relative importance of food quality compared to toxicity in predicting the fate of *Daphnia*? We predict that there will be an interaction between the two determinants of the daphnid's health, where optimal nutrition will alleviate the impacts of MeHg on neurological, reproductive, and waste management processes. However, at greater exposure, we expect that toxicity will be the dominant factor in predicting the fate of the organism.
- Can high-quality nutritional content outweigh the effects of toxicity? Following from our above prediction, we anticipate that at low to moderate MeHg concentrations, *Daphnia* will be able to ameliorate the impacts of toxicity with exposure to superior food quality.

2. Methodology

2.1. Model description

Our model consists of two components: a modified version of the individual ecophysiological sub-model (Perhar and Arhonditsis, 2015) and the predator-prey (or *Daphnia*-phytoplankton) model (Perhar et al., 2016). The individual-level daphnid model drives the predator-prey dynamics through modulation of the organism growth and grazing rate. It also considers the contents of fourteen metabolites in ingested food, where each plays a role in one or more physiological processes (see Table 1 for processes associated with each metabolite). The modelled physiological processes follow a hierarchy and can be categorized into upstream and downstream classes based on their impact. Changes to the dynamics of upstream processes have direct implications on downstream processes as bottlenecks, facilitations, or logic decisions where certain processes in the organism may switch on or off; for instance, the

Table 1
Metabolites included in our model and the physiological processes in which they are involved.

Metabolite	Abbreviation	Physiological process
Tryptophan	TRY	Neurological
Tyrosine	TYR	Neurological
Carbohydrates	CARB	Energetics
Proteins	PROT	Energetics
Fats	FAT	Energetics, osmoregulatory maintenance
Cholesterol	CLS	Osmoregulatory maintenance, anabolic growth investment
Choline	CHO	Osmoregulatory maintenance
Eicosapentaenoic Acid	EPA	Reproductive growth investment
Docosahexaenoic Acid	DHA	Reproductive growth investment
Glutamic Acid	GA	Waste management
Glycine	GLY	Waste management
Cysteine	CYS	Waste management
Phosphorus	P	Energetics, osmoregulatory maintenance, anabolic growth investment
Nitrogen	N	Nervous system, anabolic growth investment
Methylmercury	Hg	Nervous system, osmoregulatory maintenance, waste management

upstream processes (neurological functions and bio-energetics) determine the amount of energy available for downstream use, and depending on the energy available, the amount of excess metabolites to be excreted may vary. The governing differential equation for each metabolite describes the assimilated metabolite content, the mass mobilized (moving metabolites from somatic pools for physiological use) in each relevant physiological process, the mass of metabolite eliminated, and the metabolite mass contributing to organism growth (Fig. 1 and Table 2, Eqs. (57)–(70)). The predator-prey sub-model is used to describe the dynamics of *Daphnia* and phytoplankton biomass (Table 2, Eqs. (71)–(72)) (Perhar et al., 2016). The Lotka-Volterra and physiological sub-models are connected through the animal growth rate. In the Supporting information, Tables S1–S5 provide a complete list of the Lotka-Volterra parameter values, as well as the values assigned to the algal food and zooplankton somatic metabolite content, physiological rates or constants, and activation energies. The parameterization is largely based on values provided in Perhar and Arhonditsis (2015) and Perhar et al. (2016) for the metabolomics sub-model.

2.1.1. Modifications to account for MeHg impacts on zooplankton physiology

We introduce a toxicity component to the individual-level model through the inclusion of terms determining ingestion and diffusion of MeHg by *Daphnia*, which in turn directly impacts four physiological functions: neurological, osmoregulatory maintenance, waste management, and reproductive growth (Table 1). The governing differential equation for MeHg is structurally similar to those for the fourteen nutritional metabolites, and therefore considers the accumulation of MeHg in the organism from ingestion of contaminated food and dissolved uptake, the mobilization of MeHg in waste management and reproduction (Table 2, Eq. (73)). Although we do not explicitly model the excretion of MeHg, our model assumes that it is excreted concurrently with other waste as a by-product as well as though reproductive losses. Excretion of MeHg as a by-product has been observed in biological systems, although due to the chemical nature of MeHg, its complete elimination is difficult due to re-absorption through enterohepatic recirculation (Boening, 2000). The losses of MeHg in reproduction represent the transfer from somatic tissues to eggs in sexually-mature females. Several studies have found evidence of the presence of maternally-derived MeHg in daphnids as well as fish eggs (e.g., Latif et al., 2001; Tsui and Wang, 2004). Table 3 draws parallels between the physiological effects of MeHg as reported in the literature and the way accounted for by the model.

2.1.1.1. Daphnia uptake of MeHg. MeHg enters *Daphnia* through ingestion of contaminated algal food, as well as dissolved uptake from the surrounding water. Intake of MeHg from contaminated food is modelled in the same fashion as the fourteen nutritional metabolites; that is, assimilated metabolite is expressed as a function of the metabolite content in the algal food and its morphological characteristics (Perhar et al., 2016). Tsui and Wang (2004) refer to the uptake of Hg via water as dissolved uptake and their experiments showed that Hg (as Hg^{2+} and MeHg) tends to accumulate in the soft tissues of *Daphnia*. Similarly, Tsui and Wang (2007) found that Hg uptake generally increased as a function of Hg concentration within the surrounding water. Several studies have examined the uptake of Hg

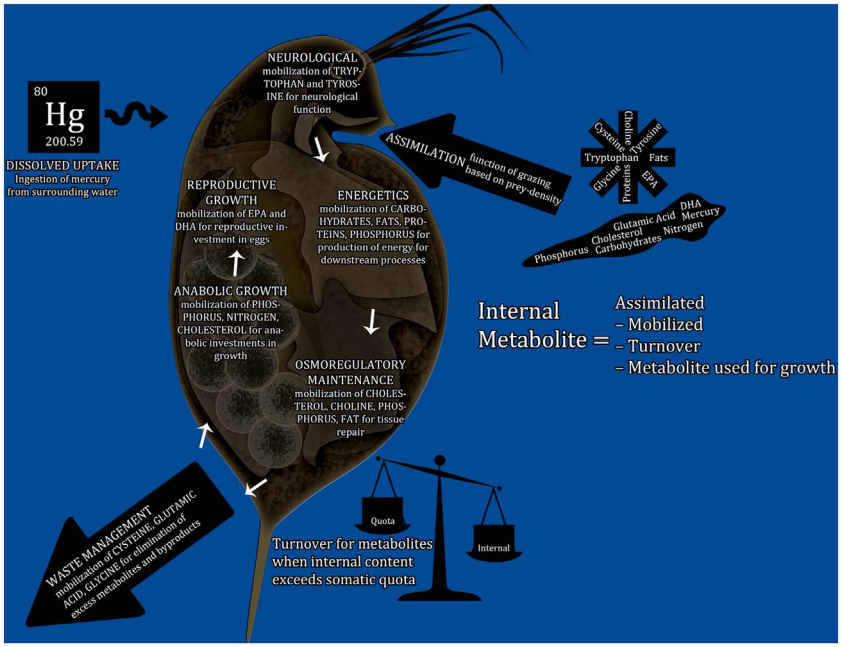

Fig. 1. Modelled physiological priorities and processes of *Daphnia*.

Table 2
Equations used to model *Daphnia* physiology, predator-prey interactions, and the impacts of methylmercury on daphnids.

1	Assimilation Efficiency (unitless) $AE = \frac{ac_1 * FQ}{ac_2 + FQ}$	38	Turnover of Excess Metabolites (Mass Excreted, μg Si mg C^{-1} day^{-1}) $Si_t = \max\left(0, \frac{Si_{int} - Si_{opt}}{Si_{opt}}\right) * \frac{availE}{\sum Si_{exceedance} * Si_{ae}} * frac$
2	Assimilation Rate (day^{-1}) $AC = graz * AE$	39	Turnover of Excess Metabolites (Energy Used, J mg C^{-1} day^{-1}) $T_{Si:C} = \max\left(0, \frac{Si_{int} - Si_{opt}}{Si_{opt}}\right) * \frac{availE}{\sum Si_{exceedance}} * frac$
3	Realized Grazing Rate (day^{-1}) $graz = grz * \frac{PREY}{PREY + h_a}$	40	Waste Management Mobilization (Cysteine Mass, μg CYS mg C^{-1} day^{-1}) $CYS_{mwas} = sat_{CYS} * \left(E_{was} * \frac{CYS_{was}}{CYS_{ae}}\right)$
4	Assimilated Metabolite (μg Si mg C^{-1} day^{-1}) $A_{Si:C} = AC * food_{Si:C}$	41	Waste Management Mobilization (Glutamic Acid Mass, μg GA mg C^{-1} day^{-1}) $GA_{mwas} = sat_{GA} * \left(E_{was} * \frac{GA_{was}}{GA_{ae}}\right)$
5	Metabolite Saturation (unitless) $sat_{Si:C} = \frac{Si_{int} - Si_{min}}{Si_{opt} - Si_{min}}$	42	Waste Management Mobilization (Glycine Mass, μg GLY mg C^{-1} day^{-1}) $GLY_{mwas} = sat_{GLY} * \left(E_{was} * \frac{GLY_{was}}{GLY_{ae}}\right)$
6	Somatic Minimum of Metabolite (μg Si mg C^{-1}) $Si_{min} = low * Si_{som}$	43	Waste Management Mobilization (Methylmercury Mass, μg Hg mg C^{-1} day^{-1}) $Hg_{mwas} = sat_{Hg} * \left(E_{was} * \frac{Hg_{was}}{Hg_{ae}}\right)$
7	Somatic Optimum of Metabolite (μg Si mg C^{-1}) $Si_{opt} = high * Si_{som}$	44	Energy Remaining for Growth (J mg C^{-1} day^{-1}) $ER = EC_2 - (E_{osm} + E_{was})$
8	Neurological Saturation (Hg Absent) (unitless) $satNEURO = \min(sat_{TRY}, sat_{TYR})$	45	Energy Allocated to Anabolic Growth (J mg C^{-1} day^{-1}) $E_{ana} = ER * EC_{ana}$
9	Neurological Saturation (Hg Present) (unitless) $satNEURO = \min(sat_{TRY}, sat_{TYR}) * e^{-k(Hg_{int} - Hg_{min})}$	46	Energy Allocated to Reproductive Growth (J mg C^{-1} day^{-1}) $E_{rep} = ER * EC_{rep}$
10	Neurological Mobilization (Tryptophan Mass, μg TRY mg C^{-1} day^{-1}) $TRY_{mneuro} = TRY_{int} * sat_{TRY} * rate_{neuro}$	47	Anabolic Growth Mobilization (Phosphorus Mass, μg P mg C^{-1} day^{-1}) $P_{mana} = sat_P * P_{growth} * \left(E_{ana} * \frac{P_{ana}}{P_{ae}}\right)$
11	Neurological Mobilization (Tyrosine Mass, μg TYR mg C^{-1} day^{-1}) $TYR_{mneuro} = TYR_{int} * sat_{TYR} * rate_{neuro}$	48	Anabolic Growth Mobilization (Nitrogen Mass, μg N mg C^{-1} day^{-1}) $N_{mana} = sat_N * N_{growth} * \left(E_{ana} * \frac{N_{ana}}{N_{ae}}\right)$
12	Neurological Mobilization (Nitrogen Mass, μg N mg C^{-1} day^{-1}) $N_{mneuro} = N_{int} * N_{neuro} * rate_{neuro}$	49	Anabolic Growth Mobilization (Cholesterol Mass, μg CLS mg C^{-1} day^{-1}) $CLS_{mana} = sat_{CLS} * CLS_{growth} * \left(E_{ana} * \frac{CLS_{ana}}{CLS_{ae}}\right)$
13	Energetic Mobilization (Carbohydrates Mass, μg CARB mg C^{-1} day^{-1}) $CARB_{mm} = sat_{NEURO} * CARB_{int} * rate_{mob}$	50	Division of Reproductive Growth (EPA Fraction, unitless) $EPA_{rep} = (1 - Hg_{rep}) * EPA_{rep}$
14	Energetic Mobilization (Fats Mass, μg FAT mg C^{-1} day^{-1}) $FAT_{mm} = sat_{NEURO} * FAT_{int} * FAT_{energy} * rate_{mob}$	51	Division of Reproductive Growth (DHA Fraction, unitless) $DHA_{rep} = (1 - Hg_{rep}) * DHA_{rep}$
15	Energetic Mobilization (Proteins Mass, μg PROT mg C^{-1} day^{-1}) $PROT_{mm} = sat_{NEURO} * PROT_{int} * rate_{mob}$	52	Reproductive Growth Mobilization (DHA Mass, μg DHA mg C^{-1} day^{-1}) $EPA_{mrep} = sat_{EPA} * \left(E_{rep} * \frac{EPA_{rep}}{EPA_{ae}}\right)$
16	Energetic Mobilization (Phosphorus Mass, μg P mg C^{-1} day^{-1}) $P_{mm} = P_{int} * P_{energy} * rate_{mob}$	53	Reproductive Growth Mobilization (EPA Mass, μg EPA mg C^{-1} day^{-1}) $DHA_{mrep} = sat_{DHA} * \left(E_{rep} * \frac{DHA_{rep}}{DHA_{ae}}\right)$
17	Energetic Mobilization (Carbohydrates Energy, J mg C^{-1} day^{-1}) $CARB_{me} = CARB_{mm} * CARB_{yield}$	54	Reproductive Growth Mobilization (Hg Mass, μg Hg mg C^{-1} day^{-1}) $Hg_{mrep} = sat_{Hg} * \left(E_{rep} * \frac{Hg_{rep}}{Hg_{ae}}\right)$
18	Energetic Mobilization (Fats Energy, J mg C^{-1} day^{-1}) $FAT_{me} = FAT_{mm} * FAT_{yield}$	55	Realized Growth Rate (day^{-1}) $growth = G_{max} * \frac{E_{ana} + E_{rep}}{E_{ana} + E_{rep} + E_{hs}}$
19	Energetic Mobilization (Proteins Energy, J mg C^{-1} day^{-1}) $PROT_{me} = PROT_{mm} * PROT_{yield}$	56	Dissolved Uptake of Hg (Hg Mass, μg Hg mg C^{-1} day^{-1}) $D_{zw} = \frac{K_{Hg} * C_w * A_z * Z_w}{B_w}$

(continued on next page)

Table 2 *(continued)*

20	Energetic Capacity (J mg C^{-1} day^{-1}) $EC = (CARB_{me} + FAT_{me} + PROT_{me})^{*}(sat_P{}^{*}P_{energy})$	57	Tryptophan Governing Equation (Tryptophan Mass, μg TRY mg C^{-1} day^{-1}) $\frac{d_{TRY}}{dt} = A_{TRY:C} - TRY_{mneuro} - TRY_t - TRY_{int}{}^{*}growth$
21	Energy Allocated to Osmoregulatory Maintenance (Hg Absent) (J mg C^{-1} day^{-1}) $E_{osm} = EC^{*}EC_{osm}$	58	Tyrosine Governing Equation (Tyrosine Mass, μg TYR mg C^{-1} day^{-1}) $\frac{d_{TYR}}{dt} = A_{TYR:C} - TYR_{mneuro} - TYR_t - TYR_{int}{}^{*}growth$
22	Energy Allocated to Methylmercury (J mg C^{-1} day^{-1}) $E_{Hg} = EC^{*}top_{Hg}$	59	Carbohydrates Governing Equation (Carbohydrates Mass, μg CARB mg C^{-1} day^{-1}) $\frac{d_{CARB}}{dt} = A_{CARB:C} - CARB_{mm} - CARB_t - CARB_{int}{}^{*}growth$
23	Energy Remaining After Allocation to Methylmercury (J mg C^{-1} day^{-1}) $EC_2 = EC - E_{Hg}$	60	Fats Governing Equation (Fats Mass, μg FAT mg C^{-1} day^{-1}) $\frac{d_{FAT}}{dt} = A_{FAT:C} - (FAT_{mm} + FAT_{mosm}) - FAT_t - FAT_{int}{}^{*}growth$
24	Energy Allocated to Osmoregulatory Maintenance (Hg Present) (J mg C^{-1} day^{-1}) $E_{osm} = EC_2{}^{*}EC_{osm}$	61	Proteins Governing Equation (Proteins Mass, μg PROT mg C^{-1} day^{-1}) $\frac{d_{PROT}}{dt} = A_{PROT:C} - PROT_{mm} - PROT_t - PROT_{int}{}^{*}growth$
25	Osmoregulatory Maintenance Mobilization (Phosphorus Mass, μg P mg C^{-1} day^{-1}) $P_{mosm} = sat_P{}^{*}P_{maint}{}^{*}\left(E_{osm}{}^{*}\frac{P_{osm}}{P_{ae}}\right)$	62	Cholesterol Governing Equation (Cholesterol Mass, μg CLS mg C^{-1} day^{-1}) $\frac{d_{CLS}}{dt} = A_{CLS:C} - (CLS_{mosm} + CLS_{mana}) - CLS_t - CLS_{int}{}^{*}growth$
26	Osmoregulatory Maintenance Mobilization (Choline Mass, μg CHO mg C^{-1} day^{-1}) $CHO_{mosm} = sat_{CHO}{}^{*}\left(E_{osm}{}^{*}\frac{CHO_{osm}}{CHO_{ae}}\right)$	63	Choline Governing Equation (Choline Mass, μg CHO mg C^{-1} day^{-1}) $\frac{d_{CHO}}{dt} = A_{CHO:C} - CHO_{mosm} - CHO_t - CHO_{int}{}^{*}growth$
27	Osmoregulatory Maintenance Mobilization (Cholesterol Mass, μg CLS mg C^{-1} day^{-1}) $CLS_{mosm} = sat_{CLS}{}^{*}CLS_{maint}{}^{*}\left(E_{osm}{}^{*}\frac{CLS_{osm}}{CLS_{ae}}\right)$	64	Eicosapentaenoic Acid (EPA) Governing Equation (EPA Mass, μg EPA mg C^{-1} day^{-1}) $\frac{d_{EPA}}{dt} = A_{EPA:C} - EPA_{mrep} - EPA_t - EPA_{int}{}^{*}growth$
28	Osmoregulatory Maintenance Mobilization (Fats Mass, μg FAT mg C^{-1} day^{-1}) $FAT_{mosm} = sat_{FAT}{}^{*}FAT_{maint}{}^{*}\left(E_{osm}{}^{*}\frac{FAT_{osm}}{FAT_{ae}}\right)$	65	Docosahexaenoic Acid (DHA) Governing Equation (DHA Mass, μg DHA mg C^{-1} day^{-1}) $\frac{d_{DHA}}{dt} = A_{DHA:C} - DHA_{mrep} - DHA_t - DHA_{int}{}^{*}growth$
29	Available Energy for Turnover (J mg C^{-1} day^{-1}) $availE = top^{*}(EC - E_{osm} - E_{was})$	66	Cysteine Governing Equation (Cysteine Mass, μg CYS mg C^{-1} day^{-1}) $\frac{d_{CYS}}{dt} = A_{CYS:C} - CYS_{mwas} - CYS_t - CYS_{int}{}^{*}growth$
30	Division of Waste Management (Cysteine Fraction, unitless) $CYS_{was} = (1 - Hg_{was})^{*}CYS_{was}$	67	Glutamic Acid Governing Equation (Glutamic Acid Mass, μg GA mg C^{-1} day^{-1}) $\frac{d_{GA}}{dt} = A_{GA:C} - GA_{mwas} - GA_t - GA_{int}{}^{*}growth$
31	Division of Waste Management (Glutamic Acid Fraction, unitless) $GA_{was} = (1 - Hg_{was})^{*}GA_{was}$	68	Glycine Governing Equation (Glycine Mass, μg GLY mg C^{-1} day^{-1}) $\frac{d_{GLY}}{dt} = A_{GLY:C} - GLY_{mwas} - GLY_t - GLY_{int}{}^{*}growth$
32	Division of Waste Management (Glycine Fraction, unitless) $GLY_{was} = (1 - Hg_{was})^{*}GLY_{was}$	69	Phosphorus Governing Equation (Phosphorus Mass, μg P mg C^{-1} day^{-1}) $\frac{d_P}{dt} = A_{P:C} - (P_{mm} + P_{mosm} + P_{mana}) - P_t - P_{int}{}^{*}growth$
33	Energy Allocated to Waste Management (Hg Present) (J mg C^{-1} day^{-1}) $E_{was} = E_{osm} + \Sigma T_{Si:C} + E_{Hg}$	70	Nitrogen Governing Equation (Nitrogen Mass, μg N mg C^{-1} day^{-1}) $\frac{d_N}{dt} = A_{N:C} - (N_{mneuro} + N_{mana}) - N_t - N_{int}{}^{*}growth$
34	Energy Allocated to Waste Management (Hg Absent) (J mg C^{-1} day^{-1}) $E_{was} = E_{osm} + \Sigma T_{Si:C}$	71	Prey Governing Equation (Prey Biomass, mg C L^{-1} day^{-1}) $\frac{d_{PREY}}{dt} = r^{*}PREY^{*}\left(1 - \frac{PREY}{K}\right) - PRED^{*}graz + inf^{*}(K - PREY)$
35	Gompertz Equation (unitless) $frac = gA^{*}e^{-gB^{*}e^{-gC^{*}\left(\frac{Si_{int} - Si_{opt}}{Si_{opt}}\right)}}$	72	Predator Biomass Governing Equation (Predator Biomass, mg C L^{-1} day^{-1}) $\frac{d_{PRED}}{dt} = growth^{*}PRED - m^{*}PRED - F^{*}\frac{PRED^2}{PRED^2 + h_z^2}$
36	Fraction of Metabolite Exceeding Somatic Optimum (unitless)	73	Methylmercury Governing Equation (Hg Mass, μg Hg mg C^{-1} day^{-1})

(continued on next page)

Table 2 *(continued)*

	$Si_{exceedance} = \frac{Si_{int} - Si_{opt}}{Si_{opt}}$	$\frac{dHg}{dt} = A_{Hg:C} - Hg_{mwas} - Hg_{mrep} + D_{zw} - Hg_{int}{}^{*}growth$
37	Fraction of Metabolite Available to Undergo Turnover (unitless) $Si_{available} = \frac{Si_{exceedance}}{\sum Si_{exceedance}}$	

from water and it has been hypothesized that facilitated transport could be an important mechanism, in addition to passive diffusion (Goldling et al., 2002; Mason et al., 1996; Moye et al., 2002; Tsui and Wang, 2004). Importantly, it was found that the mechanism of facilitated transport depends on the type of organism considered, as the uptake of Hg from water varied between prokaryotic and eukaryotic algae. We express dissolved uptake using the fugacity/aquivalence approach, which describes the behavior of a chemical in multi-media environments (e.g., Cropp et al., 2011). Our influx equation requires the area (A_Z) and biomass (B_Z) of the receiving medium (daphnid), the aquivalence capacity (Z_W) and concentration of MeHg (C_W) in the surrounding water, and a mass transfer coefficient (K_{Hg}). The final term describes the diffusion rate of the transfer of MeHg to the daphnid. Values of parameters related to dissolved uptake are presented in Table 4.

2.1.1.2. Neurological functions. In Perhar and Arhonditsis (2015) and Perhar et al. (2016), metabolite saturations were used to compare the internal concentration of a metabolite against the minimum and optimum concentration quotas; the minimum quota represents the minimum somatic requirement of the organism to survive, while exceedance of the optimum concentration requires that the daphnid allots energy to eliminate excess metabolites, divesting energy from growth. For example, the neurological saturation, a measure of the individual's capacity to synthesize neurotransmitters, was based on the minimum of the tyrosine (TYR) and tryptophan (TRY) saturations; the less saturated of the two neurological amino acids determined the neurological capacity, thus regulating subsequent downstream physiological processes. We have modified the neurological saturation to account for the effects of MeHg on the individual. When MeHg is present in the system and exceeds the lowest adverse effect level (Hg_{min}), neurological saturation exponentially declines as a function of the difference between the *Daphnia*'s internal MeHg concentration and the minimum tolerable level of MeHg; this decline restricts the downstream processes in a hierarchical manner starting with bio-energetics, reflecting the systematic impairments observed in biological systems (e.g., Fretham et al., 2012). The neurological exponential decay is governed by k (Eq. (9), Table 2), that was derived through a sensitivity analysis constrained by findings from Biesinger et al. (1982).

2.1.1.3. Bio-energetics. MeHg has an indirect effect on the bio-energetics, as this stage is driven in part by the neurological saturation upstream, and the effects of MeHg cascade downwards. With decreased neurological saturation, mobilization of energetic metabolites (CARB, FAT, PROT, P) is limited, as well as the mobilized energy through the conversion of the metabolite mass. The restricted mobilization of metabolites consequently restricts the total energetic capacity, the maximum available energy for downstream processes such as osmoregulatory maintenance, waste management, and growth investments.

2.1.1.4. Osmoregulatory maintenance. The osmoregulatory maintenance process requires phosphorus, cholesterol, choline, and dietary fats to form and repair phospholipids, membranes, and tissues. With the addition of MeHg, the energy budget changes and the majority of energy originally allocated to maintenance is redistributed to repairing the damages inflicted by MeHg. In our model, the daphnid's physiological logic prioritizes MeHg over other metabolites as the effects inflicted by MeHg may be more lethal, as compared to the typical maintenance by-products accumulated. After allocating energy to MeHg, the remaining energy for mobilization of metabolites involved in osmoregulatory maintenance is significantly reduced and divided equally among phosphorus (P), choline (CHO), cholesterol (CLS), and fats (FAT). After determining the amount of energy that is used to mobilize each metabolite, the total mass of metabolite mobilized for a process can be calculated. Consequently, with reductions to the energy allocated to metabolites, there are reductions to the mass of metabolites mobilized and thus a higher potential for them to accrue in the organism, eventually leading to metabolite super-saturation, increased stress and triggering regulatory turnover. To regulate the amount of energy allocated to dealing solely with the toxicity of MeHg in osmoregulatory maintenance processes, we introduced a constant, top_{Hg} (Table 4), which determines the fraction of the total energetic capacity that is first allocated to dealing with toxicity. As a first approximation (due to lack of data), we assumed a default top_{Hg} value of 5%.

2.1.1.5. Waste management. The high toxicity of MeHg calls for priority in excretion. Thus, in the waste management process, energy is first allocated to the excretion of MeHg and the remaining energy is divided equally among cysteine (CYS), glutamic acid (GA), and glycine (GLY). In empirical studies with fish, prolongation of the pharmacological activity of MeHg has been observed due to the reabsorption of the

Table 3
A comparison of physiological effects of methylmercury in the literature and how the model accounts for methylmercury impacts. These impacts are summarized from Fretham et al. (2012) and account primarily for observations from studies done on mammals (e.g.: rats, mice, humans).

Potential physiological impacts of methylmercury	Physiological Process	How does the model account for the impacts of methylmercury?
Neuronal cell death, decreased γ-aminobutyric acid (GABA) signalling (loss of balance of inhibition and excitation states)	Neurological	Neurological saturation reduced; neuro-metabolites cannot be fully mobilized
Impairment of electron transport chain, induction of apoptosis, DNA oxidation, elevated hydrogen peroxide levels, imbalance in oxidative state	Osmoregulatory maintenance (repair of damaged tissues)	Model first allocates osmoregulatory maintenance energy to address Hg in system; less energy for other metabolites
Bioaccumulative properties of Hg, accumulation of byproducts such as reactive oxygen species (ROS), release of cytochrome *c*	Waste management	System first allocates waste management energy to dealing with Hg; reduced turnover for other metabolites
Apoptosis	Anabolic growth Reproductive growth	Organism crippled in upstream processes through energy allocated to dealing with Hg; remaining energy for growth severely reduced

Table 4
Methylmercury parameters, values, units, and derivations. The equation numbers listed for each parameter refer to their corresponding position(s) in Table 2.

Symbol	Description	Value	Unit	Equation	Reference
K_{Hg}	Methylmercury mass-transfer coefficient	7×10^{-5}	m day^{-1}	56	Gandhi et al., 2007
B_Z	Average biomass of zooplankton	7.36×10^{-3}	mg C	56	Baudouin and Ravera, 1972
A_Z	Average area of zooplankton	6.8×10^{-7}	m^2	56	Ranta et al., 1993
C_W	Baseline ambient concentration of methylmercury in water	4.5×10^{-1}	μg Hg m^{-3}	56	Environment Canada and EPA, 2007
Z_W	Aquivalence capacity of water	1	Unitless	56	Gandhi et al., 2007
Hg_{min}	Lowest observed adverse effect level	1.84×10^{-3}	μg Hg mg C^{-1}	5, 9	Biesinger et al., 1982
Hg_{opt}	Lethal dose, 50%	1.51×10^{-1}	μg Hg mg C^{-1}	5	Biesinger et al., 1982
top_{Hg}	Maximum fraction of total energetic capacity diverted to losses associated with MeHg exposure	5×10^{-2}	Unitless	22	Present study

compound in the liver (Boening, 2000). Moreover, Boening (2000) highlights the role the excretion process can play in distributing Hg throughout the organs. To represent the bioaccumulative properties of MeHg, we prioritized the allocation of energy to MeHg removal by diverting a larger proportion of energy to mobilizing MeHg, rather than the metabolites involved in the waste management process (CYS, GA, GLY).

2.1.1.6. Growth. After the maintenance and waste management processes, the remaining energy is allocated to growth investments, divided equally among anabolic and reproductive growth. As an initial approximation due to insufficient data, we assume equal allotments of energy between anabolic and reproductive growth. MeHg exposure has been observed to lead to gradual reduction in reproductive rates (Chen and McNaught, 1992), which our model accounts for by first allocating a fraction of the remaining energy for reproductive investments to dealing with MeHg. The remaining energy after allocation to MeHg is evenly apportioned to eicosapentaenoic acid (EPA) and docosahexaenoic acid (DHA). By reserving energy to MeHg first, there is less energy remaining for reproductive investments, thus further reducing the reproductive potential of the daphnid. In lab settings, daphnid reproduction is significantly impaired at MeHg concentrations below those that significantly impact survival (Biesinger et al., 1982). Our model demonstrates this response through the physiological hierarchy, where upstream processes more critical to the organism's survival, such as neurological functions and bio-energetics are impacted first.

2.2. Model analysis

We conducted two main numerical experiments to investigate the interactive effects of food quality and MeHg content on the resistance and resilience of *Daphnia*; that is, we examined whether the consumption of high quality food could negate the detrimental effects of MeHg on daphnid growth. Specifically, we examined predator and prey population response to a 2 × 2 factorial (modelling) experiment with high and low levels of chronic exposure to MeHg (1 and 0.2 μg Hg mg C^{-1}) combined with high and low (defined as 20% of the high) neurological (TYR, TRY, N), energetic (CARB, FAT, PROT, P), and osmoregulatory (CHO, P, CLS, FAT) food quality levels (i.e., physiological processes of higher priority in our model hierarchy, and/or those mostly afflicted by MeHg exposure). The 20% change represents a balance between model functionality and the ability to produce an observable difference or effect. Toxicity and food quality were modulated by varying the quantities of MeHg and metabolites within *Daphnia* food (i.e., the algal prey) as well as the ambient water MeHg concentrations. We examined three points in time: the initial stage (t = 0 days), the transient phase (t = 5 days), and the steady state (t = 500 days). In addition, we modulated the proportions of total energy budget to addressing MeHg in the daphnid body. Specifically, we monitored changes to the total energetic capacity with different top_{Hg} values (0.05 and 0.10) to examine the consequences of allocating more or less resources to managing the MeHg impacts.

To examine the resilience of *Daphnia* to acute MeHg exposure, we monitored the predator (*Daphnia*) and prey (phytoplankton) biomasses over time to study differences during and after an exposure event. This acute exposure event involved a sudden increase at t = 150 days in algal MeHg and ambient water MeHg concentrations; we doubled algal MeHg concentrations (increase to 0.145 μg Hg mg C^{-1}), and increased water concentrations over 1500 times (increase to 710 μg Hg mg C^{-1} from 0.45 μg Hg mg C^{-1}). After 1000 days, this exposure event was removed and both water and algal MeHg concentrations returned to baseline levels. Given that the model prioritizes the neurological and energetic processes, we studied the consequences of an exposure event to prey and predator biomasses while reducing neurological and energetic food quality separately and concurrently (by increments of 4% up to a 32% reduction).

3. Results

3.1. Importance of food quality relative to toxicity on prey-predator dynamics

The increase of MeHg in phytoplankton led to negative impacts on *Daphnia* abundance, but the actual impact was modulated by the content of the various metabolites. Under low phytoplankton MeHg but increasing neurological food content, there was a slight daphnid biomass increase and phytoplankton biomass decrease (Fig. 2a, b). Concurrently, there were no changes observed with regard to the daphnid somatic MeHg under low algal MeHg content (Fig. 2c). As algal MeHg food content increased, the daphnid biomass declined rapidly past an algal MeHg threshold and remained low, despite high levels of prey biomass, while daphnid internal Hg content continued to increase. This pattern held true under all levels of neurological food content (Fig. 2a–c). The internal daphnid MeHg concentrations, which remained relatively constant up until a threshold, reflect the physiological mechanisms used to eliminate MeHg from the system, such as the increased allocation of energy within osmoregulatory maintenance and waste management towards MeHg. Prior to the exceedance of this threshold, we still observed changes to predator biomass because there was enough energy remaining for growth, after the increased investments in osmoregulatory maintenance and waste management towards MeHg. The threshold represents the tipping point at which the daphnid is no longer able to sustain itself due to the detrimental effects of toxicity outweighing the beneficial effects of food quality. After the threshold, there is neither energy for growth, nor sufficient energy to address the detrimental impacts of MeHg.

Similar patterns were observed when considering variations in food quality associated with energetic (Fig. 2d–f) and osmoregulatory maintenance metabolites (Fig. 2g–i), which were more pronounced relative to those induced by changes in neurological food quality. For example, among the three types of food quality, changes in energetic

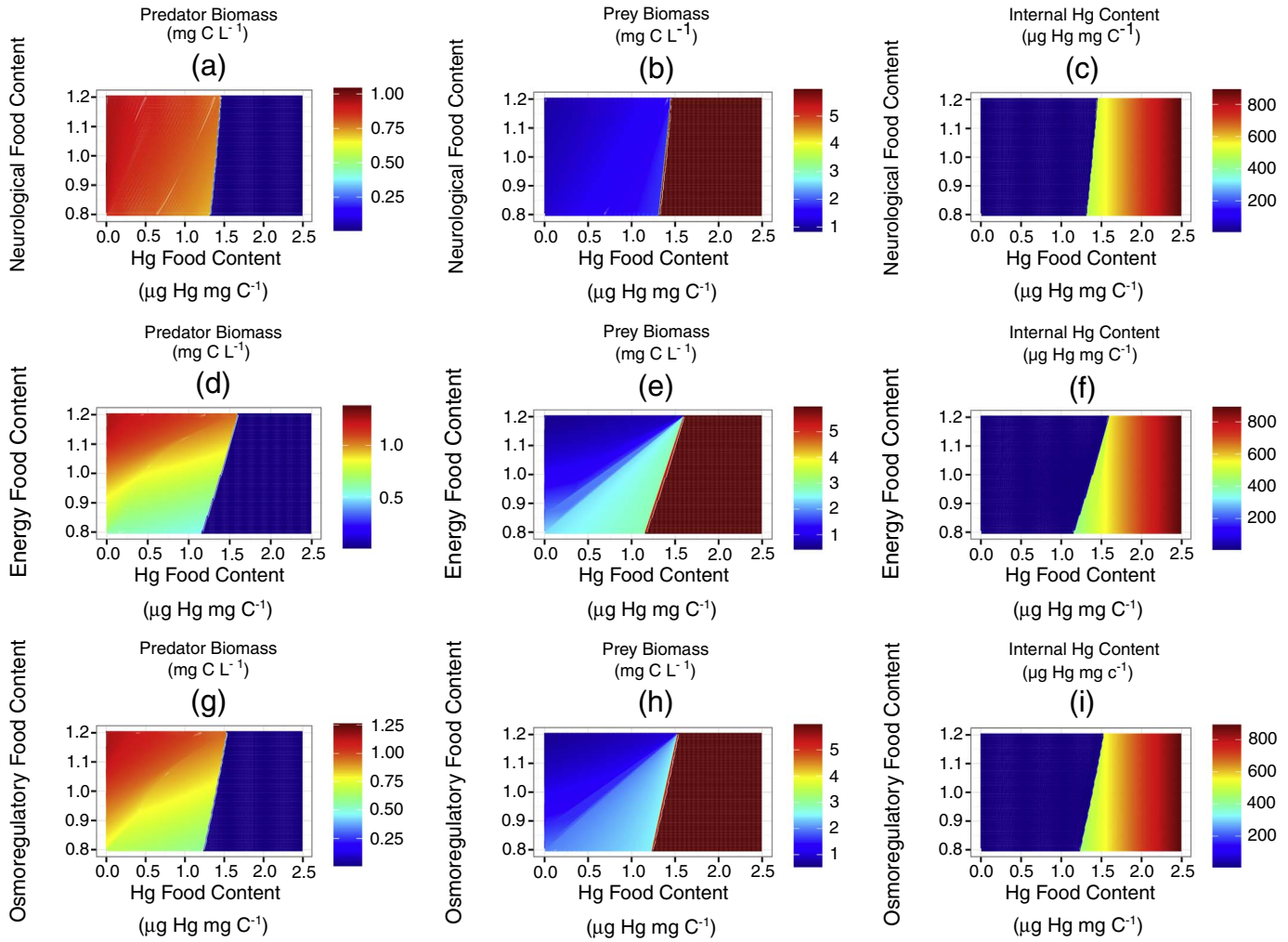

Fig. 2. Responses of predator, prey, and methylmercury content against a continuum of food nutritional quality and methylmercury food content. *Top panels* depict the response to the variation of neurological metabolites; *middle panels*, energetic metabolites; *bottom panels*, osmoregulatory maintenance metabolites. The y-axis in each panel ranges from 0.8 to 1.2, the factor by which each of the metabolites associated with the indicated process was modulated, relative to the baseline values presented in Table S2.

food quality, followed by osmoregulatory food quality, at low MeHg food content, led to the greatest relative changes in daphnid biomass (Fig. 2d, g), while internal daphnid MeHg concentrations remained constant (Fig. 2f, i). Overall, for all three types of food, we observed abrupt changes to both daphnid and phytoplankton biomass and internal daphnid MeHg concentration at threshold values of MeHg food content between 1.0 and 1.5 µg mg C^{-1}. Bearing the theoretical nature of our work in mind, it is still worth noting that these threshold values were approximately tenfold greater than the measured maximum tolerable MeHg concentration in *Daphnia* (Biesinger et al., 1982). For a given algal MeHg content, the threshold value of abrupt change was greater at higher food quality, particularly when modulating energetic food quality, which underscores the role of food quality in increasing resistance to toxicity.

3.2. Resistance of *Daphnia* to toxicity at the macroscopic level

Predator and prey biomass demonstrated different trajectories over time depending on the combinations of energetic food quality and MeHg exposure (Fig. 3). Under conditions of low energetic food quality and low MeHg food content, *Daphnia* and phytoplankton were initially at equal biomass levels, but due to the rapid decline in phytoplankton biomass during the transition phase, *Daphnia* subsequently experience a sharp biomass decline (Fig. 3a). At steady state, the phytoplankton population recovers to its initial level, while the daphnid population does not, remaining at constant but low biomass levels. At this point, although there exists a sufficient quantity of food available (i.e., high prey biomass), the low energetic quality of the available algal prey results in an insufficient amount of energy available for the daphnid population to recover to its initial state.

When MeHg food content increased but energetic food quality remained low, the pattern of daphnid and prey biomass trajectories was similar, but there was a greater difference between prey and predator biomass at steady state (i.e., t = 500), where the daphnid was almost eliminated (Fig. 3c). Conversely, under conditions of low MeHg food content but high energetic food quality, algal biomass was lower in magnitude but still greater than *Daphnia* biomass at steady state, and the predator:prey ratio was close to 1 (Fig. 3b). This pattern of predator and prey biomass trajectories was similar under conditions of high energetic food quality and high MeHg food content, although the predator:prey ratio was slightly lower at steady state conditions (Fig. 3d). Overall, exposure to MeHg led to a greater difference between predator and prey biomass at steady state, where the predator population was near depletion at high MeHg concentrations. However, as energetic food quality shifted from low to high, the daphnid population was able to sustain itself, even when exposed to MeHg through algal food. Simply put, although increased MeHg concentrations led to decreases in the daphnid population, increased food quality served as a buffer to toxicity. Our observation of a greater predator:prey ratio under high food quality and high MeHg concentrations (Fig. 3d)

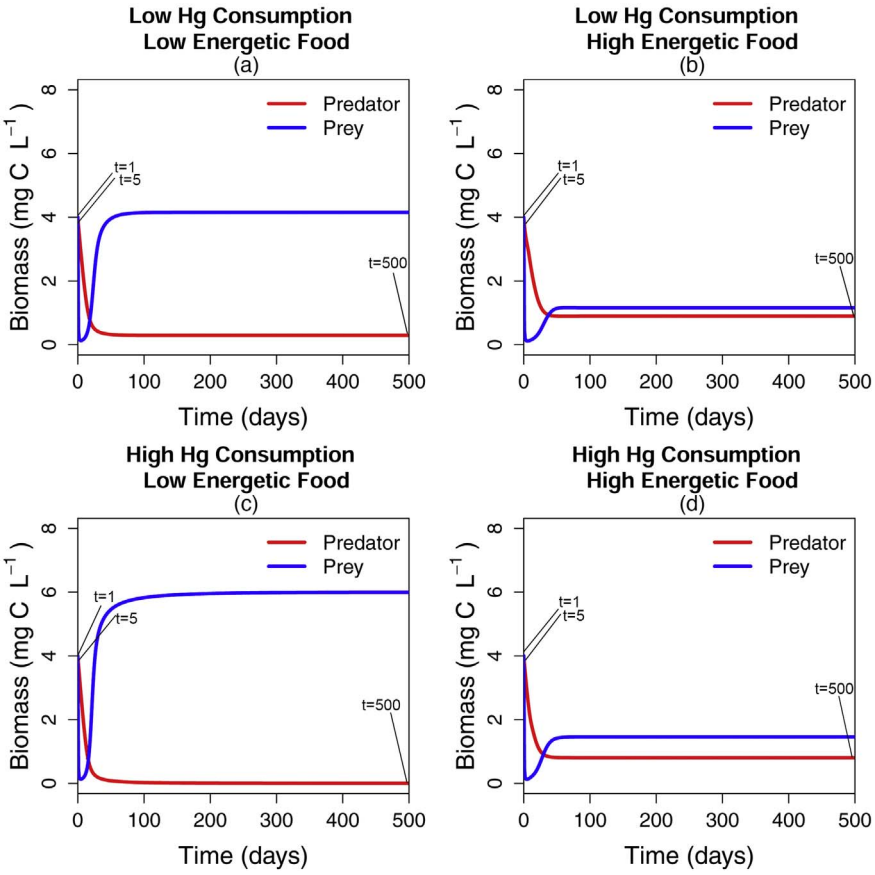

Fig. 3. Time series of predator and prey responses to different combinations of algal methylmercury concentration and energetic food content. The initial (t = 1), transition (t = 5), and steady state (t = 500) points are denoted. Four scenarios are examined with regard to food consumed by the daphnid: a) low Hg concentrations and low energetic food quality, b) low Hg concentrations and high energetic food quality, c) high Hg concentrations and low energetic food quality, and d) high Hg concentrations and high energetic food quality. Energetic metabolites (CARB, FAT, PROT, P) were at baseline values (Table S2) for high energetic food quality and half of baseline values for low energetic food quality. Hg concentrations were lowered to 0.2 μg Hg mg C^{-1} for the scenario of low Hg concentrations in algal food, while high Hg concentrations were set at 1 μg Hg mg C^{-1}.

compared to low food quality and low MeHg concentrations (Fig. 3a) is suggestive of a stronger influence of food quality, rather than quantity, in conferring resistance to toxic stress.

3.3. Resistance of Daphnia to toxicity at the intra-organismal level

In order to understand how *Daphnia*'s resistance changes in response to varying toxicity and food quality, we examined changes to phosphorus assimilation and mobilization per unit biomass at three snapshots: the initial phase (t = 1 day), the transient phase (t = 5 days), and the steady state phase (t = 500 days). Phosphorus was considered the most reflective metabolite of daphnid physiology due to its multifaceted role in various physiological processes; even within the context of our simplified representation. When *Daphnia* was exposed to low MeHg concentrations and provided low food quality, there was low assimilation, and consequently low mobilization (for bio-energetics) during the initial phase of the simulation (Fig. 4a). With *Daphnia* entering the transient phase, assimilation further decreased with a slight increase in mobilized phosphorus for energy. The daphnid also began to use phosphorus for growth (Fig. 4b). As the daphnid population achieved an equilibrium state, assimilation increased once again, as did the amount of phosphorus allocated to growth and bio-energetics (Fig. 4c). Throughout this simulation, there was no phosphorus mobilized for osmoregulatory maintenance, regulatory turnover, or anabolic investments. With energetic food quality increases in prey, increased assimilation and mobilization of metabolites occurs, along with noticeable increases in phosphorus allocated to daphnid growth. Initially, the daphnid assimilates a great deal of phosphorus, mobilizing some for bio-energetics and using a small quantity for growth (Fig. 4d). During the transient phase, assimilation decreases while there is an increase in phosphorus mobilized for bio-energetics and growth (Fig. 4e). This coincides with a sharp decrease in phytoplankton biomass, thus providing *Daphnia* with smaller amounts of high quality food (Fig. 3b). At steady state, although there is a decreased phytoplankton population relative to the initial state, the higher food quality allows for increased assimilation, greater mobilization of phosphorus for bio-energetics, and increased use of phosphorus for daphnid growth (Fig. 4f).

This pattern is consistent across the other energetic metabolites, i.e., carbohydrates, fats, and proteins (Fig. 5). Notably, the neurological metabolites, tryptophan (Fig. 5a–d) and nitrogen (Fig. 5q–t), showed a contrasting pattern of decreased assimilation with increased energetic food quality at the steady state. This decline in assimilation and consequently mobilization and use in daphnid growth stems from the decrease in prey biomass. Prey density contributes to the assimilation efficiency and ultimately to the amount of metabolite assimilated. With the energetic metabolites, this pattern was not observed because the increased energetic food quality played a greater role than the prey density. The collective profiles of the non-energetic metabolites were largely driven by assimilation efficiency (through prey density) rather than food quality. Increased energetic food quality allows *Daphnia* to mobilize more of the energetic metabolites, or in the case when maximum mobilization has already been achieved, use more metabolite for organism growth and thus greater daphnid biomass levels.

Algal MeHg content generally reduced the amount of metabolites mobilized for daphnid growth (Figs. 4, 5). With increased toxicity, less phosphorus (as well as other energetics metabolites) was used in organism growth at steady state, relative to the scenarios with low

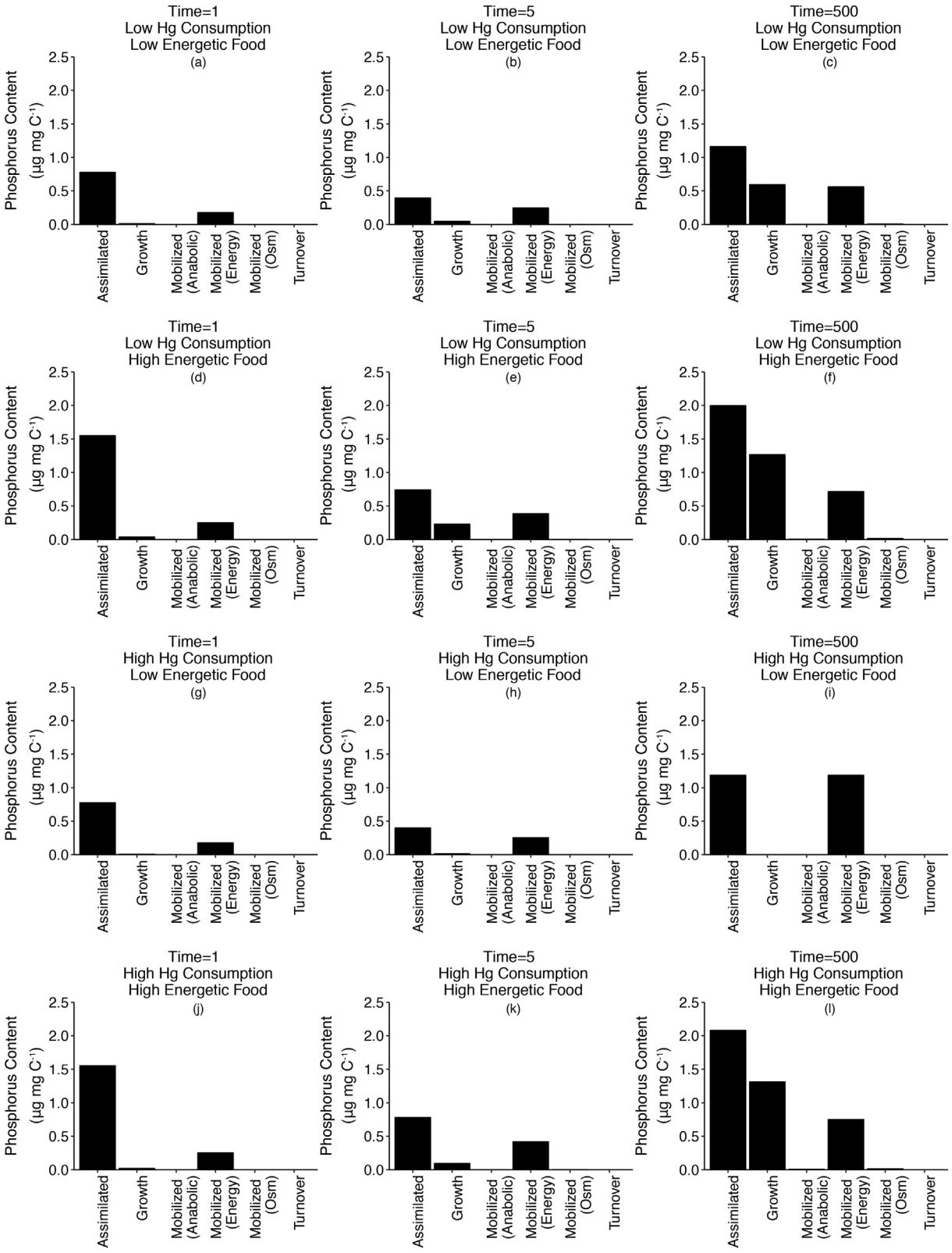

Fig. 4. Responses of select metabolites to different combinations of methylmercury food content and energetic food content at t = 1 day (initial), t = 5 days (beginning of transition), t = 500 days (steady state). Energetic metabolites (CARB, FAT, PROT, P) were at baseline values (Table S2) for high energetic food quality and half of baseline values for low energetic food quality. Hg concentrations were lowered to 0.2 µg Hg mg C^{-1} for low Hg concentrations in algal food, while high Hg concentrations were set at 1 µg Hg mg C^{-1}.

MeHg concentrations. The decline in metabolites used in organism growth stems from the elevated toxicity which impedes mobilization of metabolites through a decreased neurological saturation, and thus decreasing metabolite availability. The daphnid prioritizes metabolite mobilization for other processes and uses remaining metabolite and energy reserves for organismal growth. Thus, following the logic of our model, the daphnid is able to sustain itself in the presence of MeHg exposure only with high quality energetic food. Exposure to high MeHg

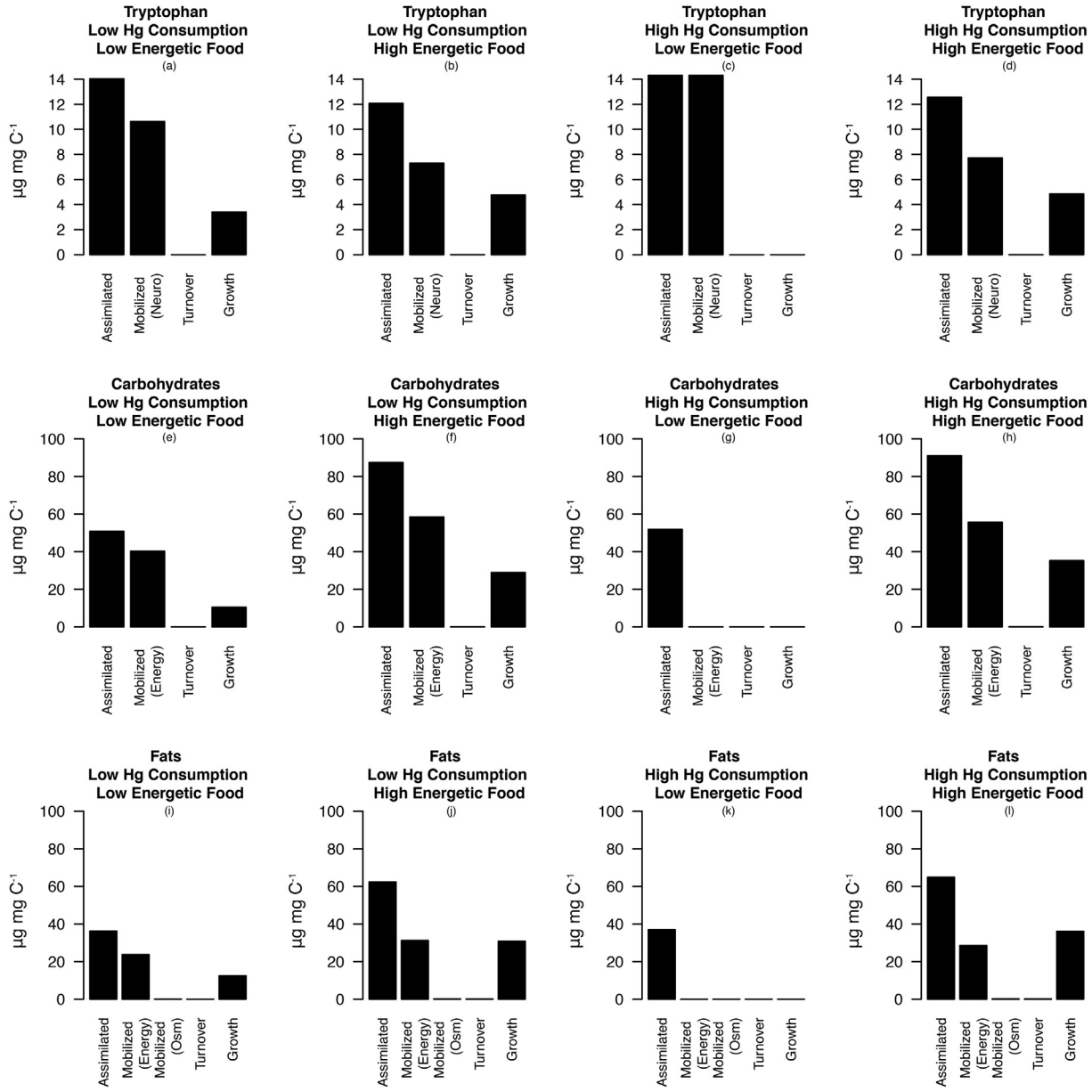

Fig. 5. Variations in the concentrations of energetic (CARB, FAT, PROT, P) and select neurological (TRY, N) metabolites to different combinations of methylmercury and energetic food content at steady state. Energetic metabolites were at baseline values (Table S2) for high energetic food quality and half of baseline values for low energetic food quality. Hg concentrations were lowered to 0.2 µg Hg mg C^{-1} for low Hg concentrations in algal food, while high Hg concentrations were set at 1 µg Hg mg C^{-1}.

concentrations and low quality food, led to the most negative impact on the health of daphnid (Fig. 4g–i; Fig. 5). At steady state, apart from the neurological compounds (tryptophan and nitrogen), there is no mobilization or use of metabolites for daphnid growth under nutritional stress and toxicity. Overall, across all numerical experiments, with exposure to toxicity, the daphnid changes its resource allocation, prioritizing maintenance over growth; increasing food quality replenishes some of the energetic costs associated with toxicity, whereby daphnids are offered additional resources for growth as well as a buffer to manage toxicity.

We introduced a term, top_{Hg}, to reflect the proportion of total energy budget allocated to eliminating the somatic MeHg and ameliorating its impacts. Energetic food quality had a greater impact on total energetic capacity, the total energy available for downstream processes (i.e., osmoregulatory maintenance, waste management, and growth) than toxicity of MeHg, regardless of the proportion of energy allocated to eliminating MeHg (Fig. 6). Under conditions of low levels of energy allocated to MeHg elimination (i.e., low top_{Hg} value), exposure to MeHg in algal food had little impact on the total energetic capacity when energetic food quality was high (Fig. 6a). However, when consuming low energetic food quality, daphnid total energetic capacity was lower and was strongly impacted under higher MeHg consumption. These patterns held true under scenarios of high energy allocation to dealing with the effects of MeHg (Fig. 6b), although the magnitude of the total energetic capacity was slightly larger across the four scenarios. Thus, regardless of the proportion of energy allocated to eliminating MeHg, the availability of higher energetic quality food led to greater increases in the total energetic capacity within the daphnid and consequently, increased resistance to MeHg toxicity.

3.4. Resilience of Daphnia to toxicity

We examined the resilience of predator and prey populations to reductions (ranging from 8%–32%) in neurological and energetic food quality, relative to the default values presented in Table S2, after an exposure event (Fig. 7). We focused on three points in the time series:

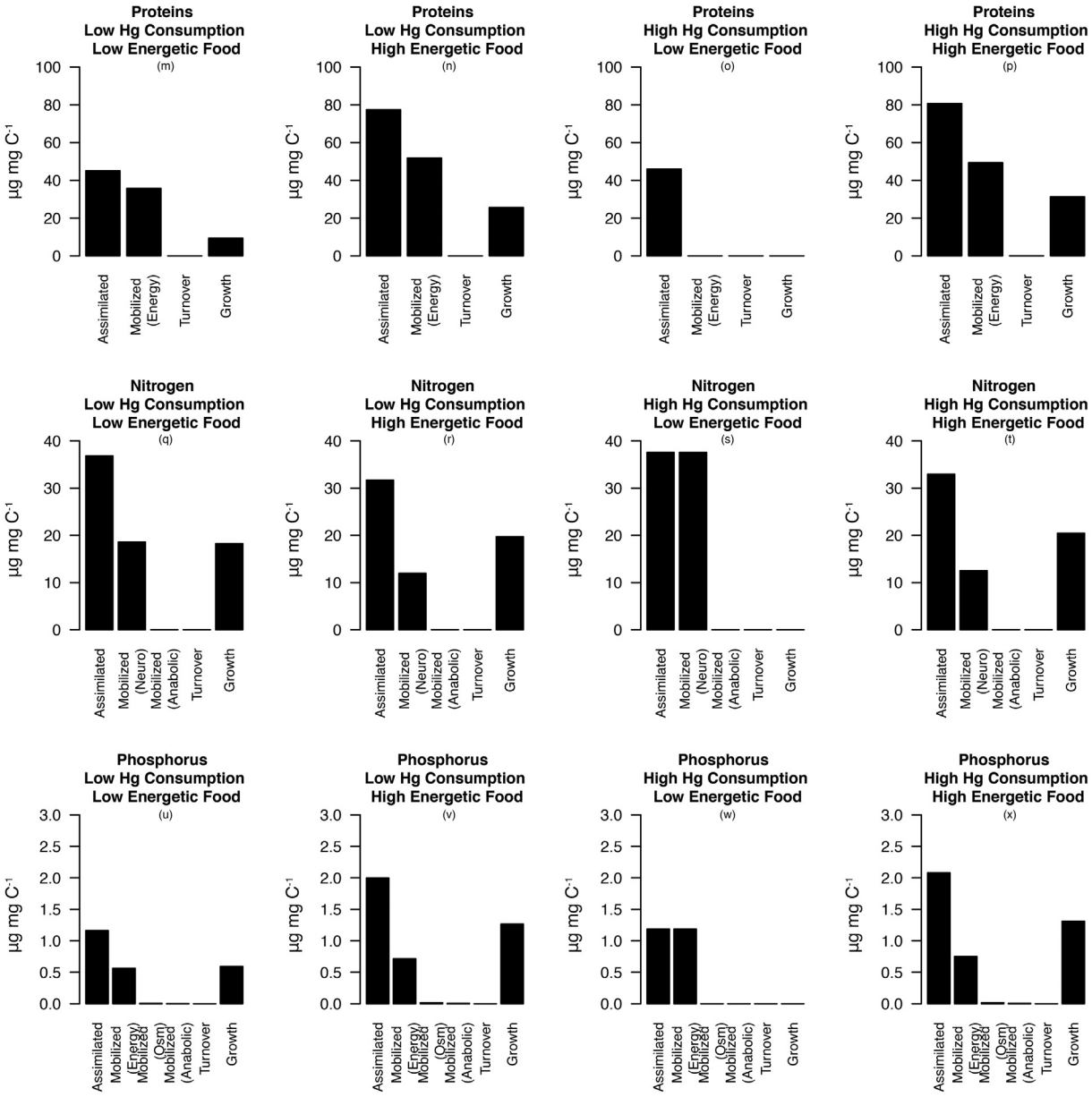

Fig. 5. (*continued*)

the initial condition prior to exposure (t = 150 days), during exposure to the toxicant (t = 500 days), and after the toxicant was removed (t = 3000 days). For these experiments, we compared changes in predator and prey biomass over time with increasing reductions in the amount of different metabolites within and between two different types of food quality (i.e., neurological, energetic food content). In addition, we examined transitions to alternative steady states (defined as an abrupt shift to a different predator:prey ratio), as well as the extent of recovery of the populations to the initial state in the post-exposure period.

We observed a high degree of daphnid population resilience with decreasing neurological food quality (see also Fig. 8). Under minimal reduction (8%) of the neurological food quality, *Daphnia* experiences a sharp decline after the exposure event (Fig. 7a). Upon the termination of the MeHg exposure, biomass levels returned to the pre-exposure levels for both daphnid and phytoplankton populations, reflecting the ability of the daphnid to sustain itself in the presence of toxicity. As neurological food quality was further reduced, the predator-prey system was still able to return to pre-exposure dynamics, except in the case of the maximum reduction tested (32% reduction), when the exposure event led to the elimination of the predator (Fig. 7j). Similar results were observed in the scenario where only energetic food quality was reduced (Fig. 7b, e, h, k). When both neurological and energetic food quality was reduced simultaneously, we observed rapid loss of top-down control of prey biomass (predator:prey < 1) which eventually led to predator elimination with the 24% and 32% reduction scenarios (Fig. 7i, l). These patterns highlight the consequences of a nutritionally inferior diet with respect to the resilience of the daphnid population and the likelihood of recovery from an exposure event. Nutritionally balanced diet is possible to ameliorate and mitigate the impacts of toxicity, even in cases of acute exposure. Interestingly, we observed abrupt, rather than gradual, transitions from daphnid-dominated to phytoplankton-dominated states between onset and termination of MeHg exposure in our numerical experiments (Fig. 8). Moreover, the content of the predator's diet in energetic metabolites appears to play a more significant role than the neurological metabolites, as the daphnid abundance in the post-exposure period reduces more rapidly for every incremental reduction of the former compounds.

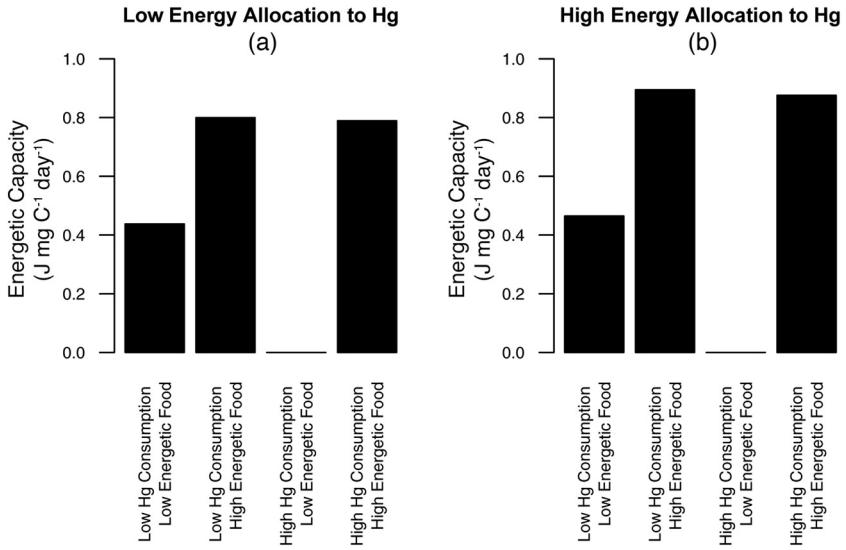

Fig. 6. Variations in total energetic capacity in response to different combinations of methylmercury food content and energetic food content, with a) low energy allocation to dealing with methylmercury and b) high energy allocation. Energetic metabolites (CARB, FAT, PROT, P) were at baseline values (Table S2) for high energetic food quality and half of baseline values for low energetic food quality. Hg concentrations were lowered to 0.2 μg Hg mg C^{-1} for low Hg concentrations in algal food, while high Hg concentrations were set at 1 μg Hg mg C^{-1}.

4. Discussion

Examples of the bio-accumulative impacts of Hg to top predators in aquatic food webs are replete in the literature (e.g., Hammerschmidt and Fitzgerald, 2006; Ward et al., 2010). Due to its chemical nature, Hg accumulates in biological media and biomagnifies, increasing in concentration with each subsequent trophic level in the ecosystem (Zananski et al., 2011). *Daphnia*, a species often used as a bio-indicator in environmental monitoring, provides insights into the state of an aquatic ecosystem, due to its role as a keystone herbivore, mediating the interactions between autotrophs (phytoplankton) and higher level predators. Toxic impairment of Hg in *Daphnia* can be particularly detrimental; Boening (2000) highlights in a review that *Daphnia* is one of the most sensitive species to Hg. Thus, due to this sensitivity, *Daphnia* serves as an excellent indicator of when the system has poor supply of organic carbon to higher trophic levels (Martin-Creuzburg et al., 2005). Herein, we applied the current understanding of biochemical and physiological impacts of MeHg in biological systems to model mechanisms by which MeHg inflicts energetic costs upon *Daphnia*. Our modelling results supported our hypotheses that at low to intermediate MeHg concentrations, high algal food quality buffers toxicity to ameliorate the toxicity effects. Moreover, we demonstrate that *Daphnia* can exhibit both resilience and resistance when exposed to MeHg up until a threshold is exceeded, when we observe a (typically abrupt) decline in daphnid biomass.

In biological systems, significant physiological impediments are induced by exposure to MeHg, such as cell death and imbalances in excitation and inhibition states of neurons, as well as imbalances in oxidative states (Fretham et al., 2012). Further, De Coen and Janssen (2003) demonstrated that under toxic stress from mercuric chloride, *D. magna* exhibited a lower content of carbohydrates, proteins, and lipids, as well as decreased energy reserved for electron transport chain activity, as would be expected due to the imbalances in oxidative states, impacting the mitochondria. In *Daphnia*, sub-lethal doses of Hg have resulted in increased activity of glycogen breakdown (De Coen et al., 2001), suggesting osmotic stress and increased energetic costs (Possik and Pause, 2016). In our model, we observed similar patterns whereby increased MeHg toxicity led to a decrease of the daphnid's total energetic capacity, as a result of decreased mobilization of energetic metabolites. Although MeHg does not explicitly target the bioenergetics process, its impacts on the neurological functions cascade downstream affecting subsequent processes. Furthermore, our model considers energetic consequences of the bioaccumulative properties of MeHg. Due to the additional stress upon *Daphnia* to eliminate the MeHg from its body, we observed additional taxes on the energetic budget which were reflected in the decreased total energetic capacity, as well as the metabolite profiles through the prioritization of mobilization over growth. Our results are conceptually on par with those reviewed by Fretham et al. (2012), which highlighted impediments to the ATP cycle, specifically in the electron transport chain.

The existing empirical literature on Hg toxicity in *Daphnia* primarily focuses on mortality and losses to fecundity (e.g., Biesinger et al., 1982; Chen and McNaught, 1992). However, critical gaps exist in our understanding of other aspects of daphnid health in relation to toxicity, such as the energetic consequences of dealing with MeHg exposure on individual (and subsequently population) growth. Furthermore, studies on *Daphnia* have typically considered its role in biomagnification, increasing body burdens in fish, and consequently impacts on human health, rather than ecosystem health. Through the application of our model, we move beyond the "fish-human health" focus towards a broader understanding of how the impacts of Hg toxicity on a physiological/individual level can manifest at the ecosystem scale. As *Daphnia* health deteriorates, its role as a predator diminishes and it is unable to maintain control over phytoplankton, allowing the autotrophs to dominate. In the presence of toxicity, the predator-prey system shifts from one dominated by top-down control to bottom-up control. The ability of *Daphnia* to resist toxic stress and recover can be linked to aquatic system resilience. Resilience studies have been performed to examine how *Daphnia* populations respond to toxic stress and return to original levels (e.g., Gergs et al., 2013; Lopes et al., 2009). The resilience of an organism depends on its buffer mechanisms which have a finite capacity; when this capacity is exceeded, resilience is lost and the system undergoes abrupt changes and possibly regime shifts (Gergs et al., 2013). Gergs et al. (2013) report that populations and systems undergo structural and internal organizational changes in their response to single stressors, which can indirectly affect their tolerance level to other stressors. Nonetheless, focusing on the risks posed by a single stressor may underestimate the actual threats to ecosystem integrity from multiple stressors. In our numerical experiments, we exposed the daphnid population to stress from toxicity as well as poor food quality. Depending on the magnitude of toxicity and nutritional stress, the interactive effects of the two factors led to significant

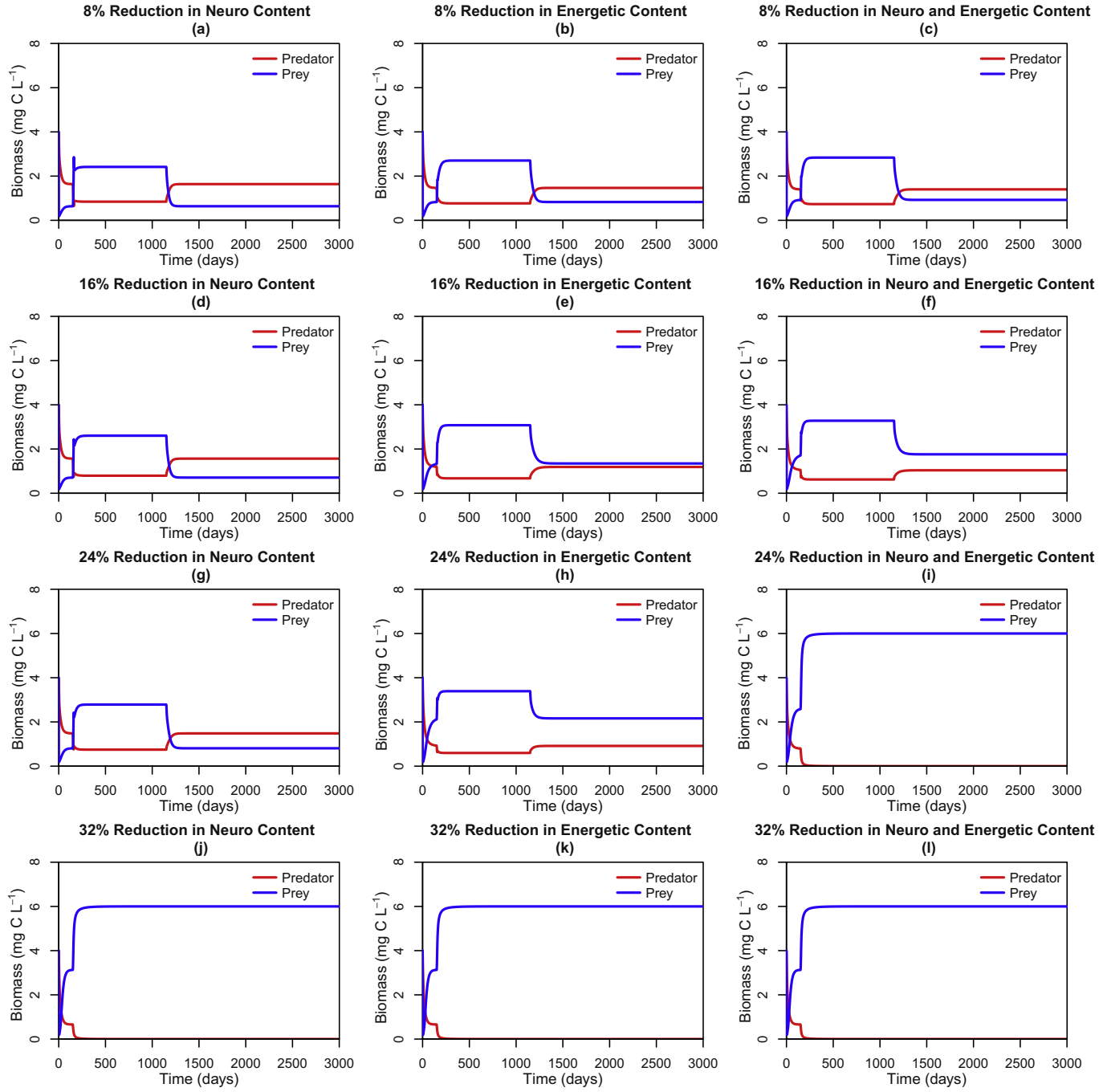

Fig. 7. Time series of the response of predator and prey biomass to reduction in food quality represented as 0–25% deficiencies in neurological and energetic metabolites. These plots capture the predator and prey populations before, during, and after exposure events, beginning at t = 150 days and ending at t = 1150 days.

differences in biomass from the perspective of both resistance and resilience.

Toxicity of Hg in biological systems has been studied in relation to many ecological and chemical variables including but not limited to trophic status (Pickhardt et al., 2002), food quality (Chapman and Chan, 2000), chlorinity (Kim et al., 2014), and temperature (Westcott and Kalff, 1996). Although nutritional quality and toxicity of food have been identified as important factors in the health of an organism (Chapman and Chan, 2000), few studies have established a relationship between MeHg and food quality, particularly for aquatic invertebrates such as *Daphnia* (e.g., Peace et al., 2016). Experimental (Biesinger et al., 1982; Chen and McNaught, 1992), as well as modelling (Huang et al., 2015) studies have typically examined the physiological consequences of Hg toxicity with little assessment of the energetic consequences of toxicity or predation. Our work addresses this knowledge gap between toxicity and nutrition in a theoretical daphnid system through incorporation of energy and mass currencies to further the understanding of energy use and allocation. Our model stipulates that upon exposure to MeHg, the daphnid is primarily crippled through its neurological functions, unable to fully mobilize neurological metabolites or use energy allocated to this process. This impediment then cascades downstream, impacting the remaining physiological processes, beginning with the bio-energetics, and subsequently osmoregulatory maintenance, waste management, and growth (anabolic and reproductive). Thus, when MeHg is present, a balance must be struck between toxicity and food quality to outweigh the detrimental effects of MeHg. Contrary to our expectation, neurological functions were not the primary point of impact of Hg toxicity in *Daphnia*, despite ranking first in our model's

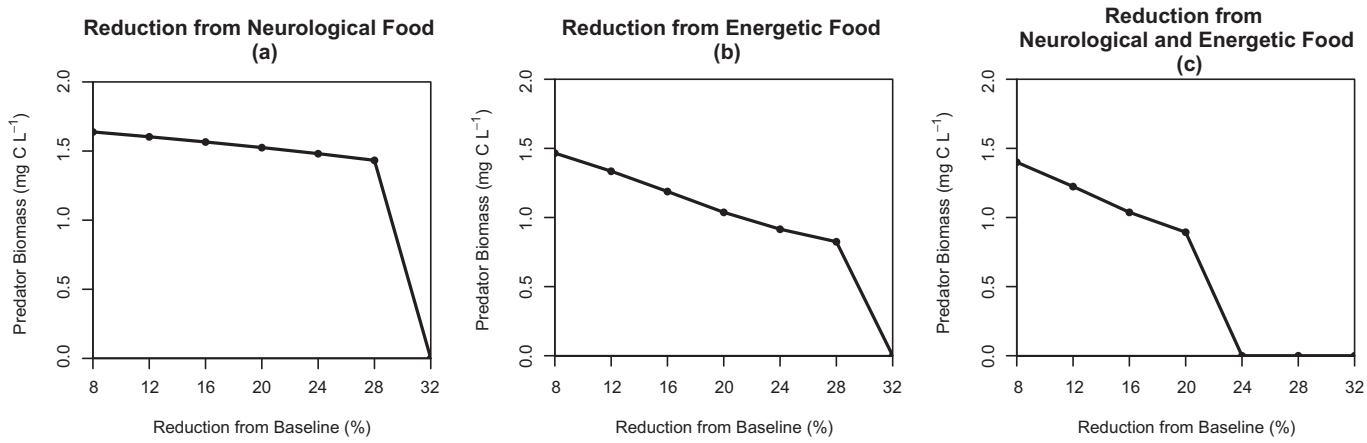

Fig. 8. Response of predator biomass to decreasing food quality in regard to a) neurological, b) energetics, and c) both neurological and energetics.

physiological hierarchy. Studies in vertebrate systems have reported significant impacts from MeHg to ATP production, specifically in the electron transport chain (one of the stages of ATP production), causing oxidative stress and imbalance (Fretham et al., 2012). Further, Fretham et al. (2012) highlight the ramifications of MeHg-induced toxicity, specifically for neurological processes, but the neurological impediments are delivered largely by cellular processes, such as impacts on the functioning of the mitochondria. Therefore, many of the neurological impairments seen in natural systems are a result of energetic losses. Our results demonstrating the relative importance of energetic food quality mirror findings from natural systems, where organismal stress from MeHg toxicity manifests primarily through energetic systems.

Much of the current modelling literature on freshwater ecology focuses on three macronutrients: carbon, nitrogen, and phosphorus (e.g., Elser et al., 2001; Peace et al., 2016). More recently, fatty acids have been identified as important mediators in the flow of mass and energy within algal communities and subsequently throughout aquatic food webs (Brett and Müller-Navarra, 1997). Fatty acids have been implicated as major factors in aquatic ecosystem health, as well as humans (Arts et al., 2001; Neff et al., 2014). Herein, we extend our focus to present the significance of a balanced multi-metabolite diet. Our work highlights the necessity of attaining food of at least a minimum quality (defined by somatic minimum quotas) in order for an individual to survive. Through our modelling analysis, we demonstrate that optimal nutrition, as defined by high quality food and a balanced composition of nutritional metabolites, can serve to ameliorate the harmful impacts of Hg toxicity. Although at high toxicity levels, death is inevitable for the daphnid under both acute and chronic exposure, we also showed that nutrition can ameliorate the repercussions of exposure at lower MeHg levels, up until a threshold where toxicity dominates. When toxicity dominates, there is a dramatic shift in the phytoplankton and *Daphnia* biomass, inducing a critical transition to an alternative state.

Our work offers a first attempt to use an ecophysiological model of *Daphnia* to examine the ramifications of exposure to MeHg toxicity on internal energy and mass budgets. Nonetheless, several limitations remain that can be used as pointers for future research. Although most parameters were sourced from literature values, a lack of data availability required us to derive others using sensitivity analysis, such as the MeHg activation energy (Hg_{ae}) and the term modulating the exponential decrease in neurological functions upon exposure to MeHg (k). However, the framework of our model accommodates parameterization based on observations from environmental metabolomics experiments. Metabolomics allow for the detection of the composition of low-weight molecules in biological media, whereby important physiological pathways can be elucidated (Alonso et al., 2015). Lankadurai et al. (2013) report in their review many instances in which metabolite data were used to infer stress based on recorded variations of metabolite compounds; for example, upon exposure to cadmium, *Daphnia* exhibits increased concentrations of glutathione, arginine, arachidonic acid, among other compounds. Using metabolite data, we can not only revisit the parameterization of our model, but also adapt its structure to account for other physiologically important metabolites as well as for the multitude of the metabolite roles in pathways.

Our prey-predator model did not consider the direct impact of Hg on phytoplankton. In our analysis, the impacts of Hg toxicity on phytoplankton are indirect, through its influence on *Daphnia*. Thus, it is likely that the effects of toxicity were underplayed, and do not reflect the actual severity on the entire ecosystem. Phytoplankton are susceptible to Hg, particularly MeHg, and experience growth inhibition (Wu and Wang, 2011). This is an aspect of toxicity that can be explored in future iterations of the model to further our understanding of toxicity in food-web dynamics. For example, Huang et al. (2015) developed a toxin-dependent, prey-predator model that explores the ramifications of toxicity on both predator and prey through direct and indirect (mediated by predator-prey interactions) effects. They found that under high concentrations, both predator and prey were impacted by toxicity. However, under intermediate toxin concentrations, predators were more heavily affected due to the role of biomagnification (Huang et al., 2015). Further consideration of toxicity to both predator and prey may allow us to emphasize and represent more accurately the ramifications of MeHg toxicity and its bioaccumulative properties in the lower food web.

Our model offers a foundation for understanding the responses of aquatic ecosystems to toxic stressors and has transferrable implications for examining the consequences of other contaminants. For example, the role of multiple contaminants may have a significant impact on resiliency. Lopes et al. (2009) found that *Daphnia* demonstrated resilience, recovering to initial densities after stress induced from exposure to mine drainage effluent containing cadmium. However, when the daphnids were successively exposed to partially lethal concentrations of a variety of contaminants, the population lost its ability to sustain itself and was eliminated, even with a sufficiently long recovery period to allow the population density to return to initial levels. Another avenue for future exploration is the interactive role of Hg and other nutrients or contaminants in algal food that may have antagonistic or synergistic effects on daphnid growth. For example, biochemical interactions between Hg and selenium may result in the formation of complexes due to Hg having a stronger affinity for selenium-containing ligands than sulfur-containing ligands (Sugiura et al., 1978). Higher levels of selenium compensate for the selenium sequestered in complexes with MeHg, to maintain regular levels of selenoenzyme activities, thereby providing antioxidant protection to the brain (Ralston et al., 2008), although the energetic ramifications of

increasing selenium concentrations are currently unknown. Other evidence suggests that elevated ambient chloride levels are associated with higher MeHg concentrations in plankton (Kim et al., 2014). In marine waters, MeHg and chloride bind to form complexes; these complexes facilitate membrane permeability and subsequently MeHg bioaccumulation (Kim et al., 2014). Moreover, interactions of polychlorinated biphenyls (PCBs) or polybrominated diphenyl ethers (PBDEs) with Hg have demonstrated additive and synergistic effects in biological systems (Fischer et al., 2008; Stavenes Andersen et al., 2009). Fischer et al. (2008) reported enhanced deleterious effects to the neurological functions in mice, where the observed effects were more than just additive. As certain congeners of PBDEs continue to increase globally (Law et al., 2014), there is value to furthering our understanding of the ecosystem-level consequences of interactive effects of contaminants in aquatic systems.

Building upon the *Daphnia* ecophysiological models developed by Perhar and Arhonditsis (2015) and Perhar et al. (2016), we present a new perspective in plankton ecology through the integration of toxicity. Our model characterizes the energetic costs to various physiological processes in response to Hg toxicity, and illuminates the importance of a balanced diet in ameliorating the ramifications of toxicity in an aquatic herbivore. We demonstrate that metabolites associated with the bio-energetics (carbohydrates, fats, proteins, and phosphorus) confer the greatest resistance and resilience to physiological changes induced by MeHg toxicity. Predator-prey dynamics can change profoundly due to the detrimental impacts of MeHg on daphnid physiology and unfavourable nutritional stoichiometry. Under conditions of poor nutrition, as well as conditions of extreme MeHg toxicity, our model demonstrates that daphnid populations may collapse and thus phytoplankton could escape intense grazing pressure. In its present form, our work is largely theoretical, but our modelling framework allows for parameterization from experimentally-derived patterns of daphnid physiology. Responses to stress are rapidly seen at the metabolic level and can be used to develop bio-indicator systems and early warning signals for environmental monitoring (e.g., García-Sevillano et al., 2015).

Acknowledgements

We thank three anonymous reviewers whose comments have strengthened our manuscript. This project has received funding support from the Krembil Foundation. Additional funding was provided by the Natural Sciences and Engineering Research Council of Canada (NSERC) through a Discovery Grant (George Arhonditsis).

Appendix A. Supplementary data

Supplementary data to this article can be found online at http://dx.doi.org/10.1016/j.ecoinf.2017.04.002.

References

Alonso, A., Marsal, S., Julià, A., 2015. Analytical methods in untargeted metabolomics: state of the art in 2015. Front. Bioeng. Biotechnol. 3, 23. http://dx.doi.org/10.3389/fbioe.2015.00023.

Arts, M.T., Ackman, R.G., Holub, B.J., 2001. "Essential fatty acids" in aquatic ecosystems: a crucial link between diet and human health and evolution. Can. J. Fish. Aquat. Sci. 58, 122–137. http://dx.doi.org/10.1139/f00-224.

Baudouin, M.F., Ravera, O., 1972. Weight, size, and chemical composition of some freshwater zooplankters: *Daphnia hyalina* (Leydig). Limnol. Oceanogr. 17, 645–649. http://dx.doi.org/10.4319/lo.1972.17.4.0645.

Biesinger, K.E., Anderson, L.E., Eaton, J.G., 1982. Chronic effects of inorganic and organic mercury on *Daphnia magna*: toxicity, accumulation, and loss. Arch. Environ. Contam. Toxicol. 11, 769–774. http://dx.doi.org/10.1007/BF01059166.

Boening, D.W., 2000. Ecological effects, transport, and fate of mercury: a general review. Chemosphere 40, 1335–1351. http://dx.doi.org/10.1016/S0045-6535(99)00283-0.

Brett, M.T., Müller-Navarra, D.C., 1997. The role of highly unsaturated fatty acids in aquatic foodweb processes. Freshw. Biol. 38, 483–499. http://dx.doi.org/10.1046/j.1365-2427.1997.00220.x.

Chapman, L., Chan, H.M., 2000. The influence of nutrition on methyl mercury intoxication. Environ. Health Perspect. 108, 29–56. http://dx.doi.org/10.1289/ehp.00108s129.

Chen, T.-Y., McNaught, D.C., 1992. Toxicity of methylmercury to *Daphnia pulex*. Bull. Environ. Contam. Toxicol. 49, 606–612. http://dx.doi.org/10.1007/BF00196306.

Chen, C., Kamman, N., Williams, J., Bugge, D., Taylor, V., Jackson, B., Miller, E., 2012. Spatial and temporal variation in mercury bioaccumulation by zooplankton in Lake Champlain (North America). Environ. Pollut. 161, 343–349. http://dx.doi.org/10.1016/j.envpol.2011.08.048.

Cropp, R., Kerr, G., Bengtson-Nash, S., Hawker, D., 2011. A dynamic biophysical fugacity model of the movement of a persistent organic pollutant in Antarctic marine food webs. Environ. Chem. 8, 263–280. http://dx.doi.org/10.1071/en10108.

De Coen, W.M., Janssen, C.R., 2003. A multivariate biomarker-based model predicting population-level responses of *Daphnia magna*. Environ. Toxicol. Chem. 22, 2195–2201. http://dx.doi.org/10.1897/02-223.

De Coen, W.M., Janssen, C.R., Segner, H., 2001. The use of biomarkers in *Daphnia magna* toxicity testing V. In vivo alterations in the carbohydrate metabolism of *Daphnia magna* exposed to sublethal concentrations of mercury and lindane. Ecotoxicol. Environ. Saf. 48, 223–234. http://dx.doi.org/10.1006/eesa.2000.2009.

Driscoll, C.T., Han, Y.-J., Chen, C.Y., Evers, D.C., Lambert, K.F., Holsen, T.M., Kamman, N.C., Munson, R.K., 2007. Mercury contamination in forest and freshwater ecosystems in the northeastern United States. Bioscience 57, 17–28. http://dx.doi.org/10.1641/B570106.

Elser, J.J., Hayakawa, K., Urabe, J., 2001. Nutrient limitation reduces food quality for zooplankton: *Daphnia* response to seston phosphorus enrichment. Ecology 82, 898. http://dx.doi.org/10.2307/2680208.

Environment Canada and the U.S. Environmental Protection Agency, 2007. State of the Great Lakes 2007. Cat No. En161-3/1-2007E-PDF. EPA 905-R-07-003. (Available at publications.gc.ca/).

Fischer, C., Fredriksson, A., Eriksson, P., 2008. Coexposure of neonatal mice to a flame retardant PBDE 99 (2,2′,4,4′,5-pentabromodiphenyl ether) and methyl mercury enhances developmental neurotoxic defects. Toxicol. Sci. 101, 275–285. http://dx.doi.org/10.1093/toxsci/kfm271.

Fretham, S.J.B., Caito, S., Martinez-Finley, E.J., Aschner, M., 2012. Mechanisms and modifiers of methylmercury-induced neurotoxicity. Toxicol. Res. (Camb.) 1, 32. http://dx.doi.org/10.1039/c2tx20010d.

Gandhi, N., Bhavsar, S.P., Diamond, M.L., Kuwabara, J.S., Marvin-DiPasquale, M., Krabbenhoft, D.P., 2007. Development of a mercury speciation, fate, and biotic uptake (BIOTRANSPEC) model: application to Lahontan Reservoir (Nevada, USA). Environ. Toxicol. Chem. 26 (11), 2260–2273. http://dx.doi.org/10.1897/06-468R.1/.

García-Sevillano, M.A., García-Barrera, T., Navarro, F., Abril, N., Pueyo, C., López-Barea, J., Gómez-Ariza, J.L., 2014. Use of metallomics and metabolomics to assess metal pollution in Doñana National Park (SW Spain). Environ. Sci. Technol. 48, 7747–7755. http://dx.doi.org/10.1021/es4057938.

García-Sevillano, M.Á, García-Barrera, T., Gómez-Ariza, J.L., 2015. Environmental metabolomics: biological markers for metal toxicity. Electrophoresis 36, 2348–2365. http://dx.doi.org/10.1002/elps.201500052/.

Gergs, A., Zenker, A., Grimm, V., Preuss, T.G., 2013. Chemical and natural stressors combined: from cryptic effects to population extinction. Sci. Rep. 3, 2036. http://dx.doi.org/10.1038/srep02036.

Gilbertson, M., Carpenter, D.O., 2004. An ecosystem approach to the health effects of mercury in the Great Lakes basin ecosystem. Environ. Res. 95, 240–246. http://dx.doi.org/10.1016/j.envres.2004.02.015.

Goldling, G.R., Kelly, C.A., Sparling, R., Loewen, P.C., Rudd, J.W.M., Barkay, T., 2002. Evidence for facilitated uptake of Hg(II) by *Vibrio anguillarum* and *Escherichia coli* under anaerobic and aerobic conditions. Limnol. Oceanogr. 47, 967–975. http://dx.doi.org/10.4319/lo.2002.47.4.0967.

Hammerschmidt, C.R., Fitzgerald, W.F., 2006. Bioaccumulation and trophic transfer of methylmercury in Long Island Sound. Arch. Environ. Contam. Toxicol. 51, 416–424. http://dx.doi.org/10.1007/s00244-005-0265-7.

Heathcote, A., Filstrup, C., Kendall, D., Downing, J., 2016. Biomass pyramids in lake plankton: influence of Cyanobacteria size and abundance. Inland Waters 6, 2–6. http://dx.doi.org/10.5268/IW-6.2.941.

Huang, Q., Wang, H., Lewis, M.A., 2015. The impact of environmental toxins on predator-prey dynamics. J. Theor. Biol. 378, 12–30. http://dx.doi.org/10.1016/j.jtbi.2015.04.019.

Karimi, R., Chen, C.Y., Pickhardt, P.C., Fisher, N.S., Folt, C.L., 2007. Stoichiometric controls of mercury dilution by growth. Proc. Natl. Acad. Sci. U. S. A. 104, 7477–7482. http://dx.doi.org/10.1073/pnas.0611261104.

Kim, H., Duong, H. Van, Kim, E., Lee, B.-G., Han, S., 2014. Effects of phytoplankton cell size and chloride concentration on the bioaccumulation of methylmercury in marine phytoplankton. Environ. Toxicol. 29, 936–941. http://dx.doi.org/10.1002/tox.

Lankadurai, B.P., Nagato, E.G., Simpson, M.J., 2013. Environmental metabolomics: an emerging approach to study organism responses to environmental stressors. Environ. Rev. 21, 180–205. http://dx.doi.org/10.1139/er-2013-0011.

Latif, M.A., Bodaly, R.A., Johnston, T.A., Fudge, R.J.P., 2001. Effects of environmental and maternally derived methylmercury on the embryonic and larval stages of walleye (*Stizostedion vitreum*). Environ. Pollut. 111, 139–148. http://dx.doi.org/10.1016/S0269-7491(99)00330-9.

Law, R.J., Covaci, A., Harrad, S., Herzke, D., Abdallah, M.A.E., Fernie, K., Toms, L.M.L., Takigami, H., 2014. Levels and trends of PBDEs and HBCDs in the global environment: status at the end of 2012. Environ. Int. 65, 147–158. http://dx.doi.org/10.1016/j.envint.2014.01.006.

Lopes, I., Martins, N., Baird, D.J., Ribeiro, R., 2009. Genetic erosion and population resilience in *Daphnia longispina* O.F. Müller under simulated predation and metal pressures. Environ. Toxicol. Chem. 28, 1912–1919. http://dx.doi.org/10.1897/08-

359.1.
Martin-Creuzburg, D., Wacker, A., Von Elert, E., 2005. Life history consequences of sterol availability in the aquatic keystone species *Daphnia*. Oecologia 144, 362–372. http://dx.doi.org/10.1007/s00442-005-0090-8.
Mason, R.P., Reinfelder, J.R., Morel, F.M.M., 1996. Uptake, toxicity, and trophic transfer of mercury in a coastal diatom. Environ. Sci. Technol. 30, 1835–1845. http://dx.doi.org/10.1021/es950373d.
Miner, B.E., De Meester, L., Pfrender, M.E., Lampert, W., Hairston, N.G., 2012. Linking genes to communities and ecosystems: *Daphnia* as an ecogenomic model. Proc. R. Soc. B Biol. Sci. 279, 1873–1882. http://dx.doi.org/10.1098/rspb.2011.2404.
Moye, H.A., Miles, C.J., Phlips, E.J., Sargent, B., Merritt, K.K., 2002. Kinetics and uptake mechanisms for monomethylmercury between freshwater algae and water. Environ. Sci. Technol. 36, 3550–3555. http://dx.doi.org/10.1021/es011421z.
Nagato, E.G., D'eon, J.C., Lankadurai, B.P., Poirier, D.G., Reiner, E.J., Simpson, A.J., Simpson, M.J., 2013. 1H NMR-based metabolomics investigation of *Daphnia magna* responses to sub-lethal exposure to arsenic, copper and lithium. Chemosphere 93, 331–337. http://dx.doi.org/10.1016/j.chemosphere.2013.04.085.
Neff, M.R., Bhavsar, S.P., Ni, F.J., Carpenter, D.O., Drouillard, K., Fisk, A.T., Arts, M.T., 2014. Risk-benefit of consuming Lake Erie fish. Environ. Res. 134, 57–65. http://dx.doi.org/10.1016/j.envres.2014.05.025.
Peace, A., Poteat, M.D., Wang, H., 2016. Somatic growth dilution of a toxicant in a predator–prey model under stoichiometric constraints. J. Theor. Biol. 407, 198–211. http://dx.doi.org/10.1016/j.jtbi.2016.07.036.
Perhar, G., Arhonditsis, G.B., 2015. Development of a metabolite-driven *Daphnia* ecophysiological model. Eco. Inform. 30, 82–96. http://dx.doi.org/10.1016/j.ecoinf.2015.09.002.
Perhar, G., Kelly, N.E., Ni, F.J., Simpson, M.J., Simpson, A.J., Arhonditsis, G.B., 2016. Using *Daphnia* physiology to drive food web dynamics: a theoretical revisit of Lotka-Volterra models. Eco. Inform. 35, 29–42. http://dx.doi.org/10.1016/j.ecoinf.2016.07.001.
Pickhardt, P.C., Fisher, N.S., 2007. Accumulation of inorganic and methylmercury by freshwater phytoplankton in two contrasting water bodies. Environ. Sci. Technol. 41, 125–131. http://dx.doi.org/10.1021/es060966w.
Pickhardt, P.C., Folt, C.L., Chen, C.Y., Klaue, B., Blum, J.D., 2002. Algal blooms reduce the uptake of toxic methylmercury in freshwater food webs. Proc. Natl. Acad. Sci. U. S. A. 99, 4419–4423. http://dx.doi.org/10.1073/pnas.072531099.
Pickhardt, P.C., Folt, C.L., Chen, C.Y., Klaue, B., Blum, J.D., 2005. Impacts of zooplankton composition and algal enrichment on the accumulation of mercury in an experimental freshwater food web. Sci. Total Environ. 339, 89–101. http://dx.doi.org/10.1016/j.scitotenv.2004.07.025.
Possik, E., Pause, A., 2016. Glycogen: a must have storage to survive stressful emergencies. Worm 5, e1156831. http://dx.doi.org/10.1080/21624054.2016.1156831.
Ralston, N.V.C., Ralston, C.R., Blackwell, J.L., Raymond, L.J., 2008. Dietary and tissue selenium in relation to methylmercury toxicity. Neurotoxicology 29, 802–811. http://dx.doi.org/10.1016/j.neuro.2008.07.007.
Ranta, E., Bengtsson, J., McManus, J., 1993. Growth, size, and shape of *Daphnia longispina*, *D. magna*, and *D. pulex*. Ann. Zool. Fenn. 30, 299–311.
Rolfhus, K.R., Hall, B.D., Monson, B.A., Paterson, M.J., Jeremiason, J.D., 2011. Assessment of mercury bioaccumulation within the pelagic food web of lakes in the western Great Lakes region. Ecotoxicology 20, 1520–1529. http://dx.doi.org/10.1007/s10646-011-0733-y.
Roos, D.H., Puntel, R.L., Lugokenski, T.H., Ineu, R.P., Bohrer, D., Burger, M.E., Franco, J.L., Farina, M., Aschner, M., Rocha, J.B.T., De Vargas Barbosa, N.B., 2010. Complex methylmercury-cysteine alters mercury accumulation in different tissues of mice. Basic Clin. Pharmacol. Toxicol. 107, 789–792. http://dx.doi.org/10.1111/j.1742-7843.2010.00577.x.
Stavenes Andersen, I., Voie, Ø.A., Fonnum, F., Mariussen, E., 2009. Effects of methyl mercury in combination with polychlorinated biphenyls and brominated flame retardants on the uptake of glutamate in rat brain synaptosomes: a mathematical approach for the study of mixtures. Toxicol. Sci. 112, 175–184. http://dx.doi.org/10.1093/toxsci/kfp178.
Sugiura, Y., Tamai, Y., Tanaka, H., 1978. Selenium protection against mercury toxicity: high binding affinity of methylmercury by selenium-containing ligands in comparison with sulfur-containing ligands. Bioinorg. Chem. 9, 167–180. http://dx.doi.org/10.1016/S0006-3061(00)80288-4.
Tsui, M.T.K., Wang, W.X., 2004. Uptake and elimination routes of inorganic mercury and methylmercury in *Daphnia magna*. Environ. Sci. Technol. 38, 808–816. http://dx.doi.org/10.1021/es034638x.
Tsui, M.T.-K., Wang, W.-X., 2007. Biokinetics and tolerance development of toxic metals in *Daphnia magna*. Environ. Toxicol. Chem. 26 (5), 1023–1032. http://dx.doi.org/10.1897/06-430R.1/.
Ward, D.M., Nislow, K.H., Folt, C.L., 2010. Bioaccumulation syndrome: identifying factors that make some stream food webs prone to elevated mercury bioaccumulation. Ann. N. Y. Acad. Sci. 1195, 62–83. http://dx.doi.org/10.1111/j.1749-6632.2010.05456.x.
Watras, C.J., Back, R.C., Halvorsen, S., Hudson, R.J.M., Morrison, K.A., Wente, S.P., 1998. Bioaccumulation of mercury in pelagic freshwater food webs. Sci. Total Environ. 219, 183–208. http://dx.doi.org/10.1016/S0048-9697(98)00228-9.
Westcott, K., Kalff, J., 1996. Environmental factors affecting methyl mercury accumulation in zooplankton. Can. J. Fish. Aquat. Sci. 53, 2221–2228. http://dx.doi.org/10.1139/cjfas-53-10-2221.
Wu, Y., Wang, W.X., 2011. Accumulation, subcellular distribution and toxicity of inorganic mercury and methylmercury in marine phytoplankton. Environ. Pollut. 159, 3097–3105. http://dx.doi.org/10.1016/j.envpol.2011.04.012.
Zananski, T.J., Holsen, T.M., Hopke, P.K., Crimmins, B.S., 2011. Mercury temporal trends in top predator fish of the Laurentian Great Lakes. Ecotoxicology 20, 1568–1576. http://dx.doi.org/10.1007/s10646-011-0751-9.

TOWARDS THE DEVELOPMENT OF AN ECOPHYSIOLOGICAL *DAPHNIA* MODEL TO EXAMINE EFFECTS OF TOXICITY AND NUTRITION

[SUPPORTING INFORMATION]

Felicity J. Ni, Noreen E. Kelly, George B. Arhonditsis*

Department of Physical and Environmental Sciences, University of Toronto.

1065 Military Trail, Toronto, Ontario, M1C 1A4, Canada

* Corresponding author

E-mail: georgea@utsc.utoronto.ca, Tel.: +1 416 208 4858; Fax: +1 416 287 7279.

Table S1: Lotka-Volterra sub-model parameters, values, units, and derivations. The equation each parameter corresponds to is indicated in reference to Table 2.

SYMBOL	*DESCRIPTION*	*VALUE*	*UNIT*	*EQUATION*
r	Maximum growth rate of phytoplankton	1.2	day^{-1}	71
K	Carrying capacity	6	mg C L^{-1}	71
h_a	Half-saturation constant of zooplankton	0.28	mg C L^{-1}	71
h_z	Half-saturation constant of fish	0.95	mg C L^{-1}	3
grz	Maximum grazing rate of zooplankton	0.95	day^{-1}	3
F	Fish predation rate	0.25	day^{-1}	72
inf	Diffusive inflow	0.01	day^{-1}	71
m	Zooplankton mortality rate	0.15	day^{-1}	72
G_{max}	Maximum growth rate of zooplankton	0.8	day^{-1}	55

Table S2: Algal food content expressed in µg of metabolite per mg of carbon.

SYMBOL	*DESCRIPTION*	*VALUE*	*UNIT*
$food_{TRY}$	Tryptophan availability in algal food	19.60244	µg TRY mg C^{-1}
$food_{TYR}$	Tyrosine availability in algal food	23.37945	µg TYR mg C^{-1}
$food_{CARB}$	Carbohydrates availability in algal food	141.9995	µg CARB mg C^{-1}
$food_{FAT}$	Fats availability in algal food	101.1726	µg FAT mg C^{-1}
$food_{PROT}$	Proteins availability in algal food	125.7465	µg PROT mg C^{-1}
$food_{CLS}$	Cholesterol availability in algal food	11.96645	µg CLS mg C^{-1}
$food_{CHO}$	Choline availability in algal food	5.800841	µg CHO mg C^{-1}
$food_{EPA}$	EPA availability in algal food	12.07125	µg EPA mg C^{-1}
$food_{DHA}$	DHA availability in algal food	1.577996	µg DHA mg C^{-1}
$food_{CYS}$	Cysteine availability in algal food	10.15055	µg CYS mg C^{-1}
$food_{GA}$	Glutamic acid availability in algal food	14.72672	µg GA mg C^{-1}
$food_{GLY}$	Glycine availability in algal food	2.364709	µg GLY mg C^{-1}
$food_{P}$	Phosphorus availability in algal food	3.245442	µg P mg C^{-1}
$food_{N}$	Nitrogen availability in algal food	51.44691	µg N mg C^{-1}
$food_{Hg}$	Methylmercury availability in algal food	0.145	µg Hg mg C^{-1}

Table S3: Somatic metabolite values used to calculate somatic optimum and minimum quotas of each metabolite.

SYMBOL	*DESCRIPTION*	*VALUE*	*UNIT*
som_{TRY}	Somatic tryptophan to carbon quota	21.71731	µg TRY mg C^{-1}
som_{TYR}	Somatic tyrosine to carbon quota	23.67993	µg TYR mg C^{-1}
som_{CARB}	Somatic carbohydrates to carbon quota	130.2986	µg CARB mg C^{-1}
som_{FAT}	Somatic fats to carbon quota	130.5976	µg FAT mg C^{-1}
som_{PROT}	Somatic proteins to carbon quota	158.1846	µg PROT mg C^{-1}
som_{CLS}	Somatic cholesterol to carbon quota	25.30872	µg CLS mg C^{-1}
som_{CHO}	Somatic choline to carbon quota	9.685042	µg CHO mg C^{-1}
som_{EPA}	Somatic EPA to carbon quota	24.63651	µg EPA mg C^{-1}
som_{DHA}	Somatic DHA to carbon quota	2.799227	µg DHA mg C^{-1}
som_{CYS}	Somatic cysteine to carbon quota	17.33878	µg CYS mg C^{-1}
som_{GA}	Somatic glutamic acid to carbon quota	43.06455	µg GA mg C^{-1}
som_{GLY}	Somatic glycine to carbon quota	5.163825	µg GLY mg C^{-1}
som_{P}	Somatic phosphorus to carbon quota	8.741006	µg P mg C^{-1}
som_{N}	Somatic nitrogen to carbon quota	77.991774	µg N mg C^{-1}

Table S4: Rates, constants, and fractions. The equations each parameter corresponds with are indicated in reference to Table 2.

SYMBOL	*DESCRIPTION*	*VALUE*	*UNIT*	*EQUATION*
ac_1	Thermodynamic constraint 1	0.9	unitless	1
ac_2	Thermodynamic constraint 2	0.03	$(mg\ C\ m^{-3})^{-½}$	1
FQ	Morphological food quality	0.5	$(mg\ C\ m^{-3})^{-½}$	1
low	Factor to calculate somatic minimum bounds	0.1	unitless	6
high	Factor to calculate somatic maximum bounds	1.25	unitless	7
$rate_{neuro}$	Neurological metabolite mobilization rate	0.171306	day^{-1}	10, 11, 12
$rate_{mob}$	Energetic metabolite mobilization rate	0.242061	day^{-1}	13, 14, 15, 16
N_{neuro}	Fraction of nitrogen for neurotransmitter synthesis	0.5	unitless	12
FAT_{energy}	Fraction of fat for energetics	0.5	unitless	14
P_{energy}	Fraction of phosphorus for energetics	0.33	unitless	16, 20
$CARB_{yield}$	Energetic yield of carbohydrates	0.0167	$J\ \mu g\ CARB^{-1}$	17
FAT_{yield}	Energetic yield of fats	0.0377	$J\ \mu g\ FAT^{-1}$	18
$PROT_{yield}$	Energetic yield of proteins	0.0167	$J\ \mu g\ PROT^{-1}$	19
EC_{osm}	Fraction of total energy for maintenance	0.35	unitless	21
EC_{ana}	Fraction of total energy for anabolic growth	0.5	unitless	45
EC_{rep}	Fraction of total energy for reproductive growth	0.5	unitless	46
P_{maint}	Fraction of phosphorus for maintenance	0.33	unitless	25

P_{osm}	Fraction of maintenance energy allotted to phosphorus	0.25	unitless	25
CHO_{osm}	Fraction of maintenance energy allotted to choline	0.25	unitless	26
CLS_{maint}	Fraction of cholesterol for maintenance	0.5	unitless	27
CLS_{osm}	Fraction of maintenance energy allotted to cholesterol	0.25	unitless	27
FAT_{maint}	Fraction of fats for maintenance	0.5	unitless	28
FAT_{osm}	Fraction of maintenance energy allotted to fats	0.25	unitless	28
top	Maximum fraction of growth energy diverted to homeostatic turnover	0.25	unitless	29
CYS_{was}	Fraction of waste management energy allotted to cysteine	0.33	unitless	30, 40
GA_{was}	Fraction of waste management energy allotted to glutamic acid	0.33	unitless	31. 41
GLY_{was}	Fraction of waste management energy allotted to glycine	0.33	unitless	32. 42
gA	Gompertz function constant	1	unitless	35
gB	Gompertz function constant	5	unitless	35
gC	Gompertz function constant	2	unitless	35
E_{hs}	Use efficiency of energy allotted to anabolic and reproductive growth	0.75	mg C m^{-3}	55

Table S5: Metabolite activation energies.

SYMBOL	*DESCRIPTION*	*VALUE*	*UNIT*
TRY_{ae}	Tryptophan activation energy	0.00070509831	J μg TRY^{-1}
TYR_{ae}	Tyrosine activation energy	0.00070606185	J μg TYR^{-1}
$CARB_{ae}$	Carbohydrates activation energy	0.00056476809	J μg $CARB^{-1}$
FAT_{ae}	Fats activation energy	0.0003157469	J μg FAT^{-1}
$PROT_{ae}$	Protein activation energy	0.00028106825	J μg $PROT^{-1}$
CLS_{ae}	Cholesterol activation energy	0.000018141122	J μg CLS^{-1}
CHO_{ae}	Choline activation energy	0.00079870214	J μg CHO^{-1}
EPA_{ae}	EPA activation energy	0.00013623744	J μg EPA^{-1}
DHA_{ae}	DHA activation energy	0.00011221653	J μg DHA^{-1}
CYS_{ae}	Cysteine activation energy	0.00072832288	J μg CYS^{-1}
GA_{ae}	Glutamic acid activation energy	0.00030302878	J μg GA^{-1}
GLY_{ae}	Glycine activation energy	0.00053084562	J μg GLY^{-1}
P_{ae}	Phosphorus activation energy	0.00129	J μg P^{-1}
N_{ae}	Nitrogen activation energy	0.00249	J μg N^{-1}